

Light curve "hiccups" caused by accretion column switching stellar hemisphere

Miljenko Čemeljić, 席門傑

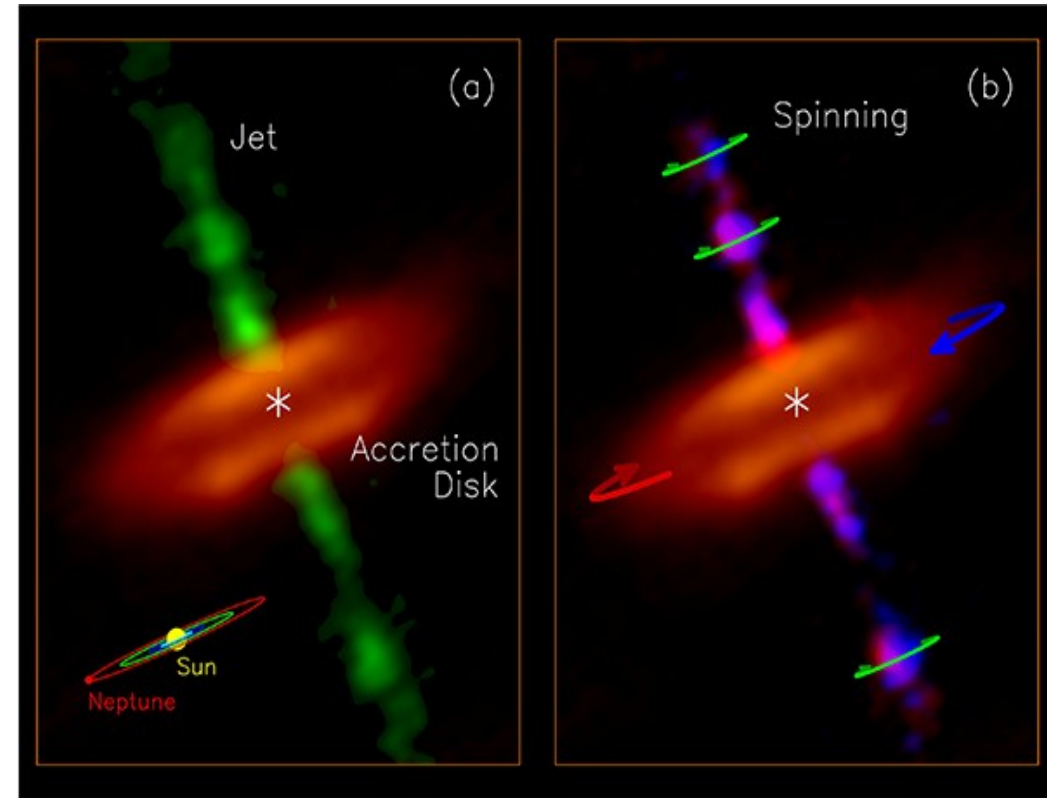
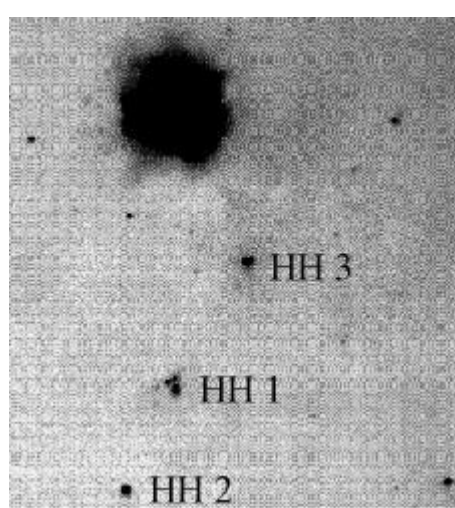
Nicolaus Copernicus Astronomical Center, Warsaw, Poland

Academia Sinica Institute of Astronomy and Astrophysics, Taipei, Taiwan

Outline

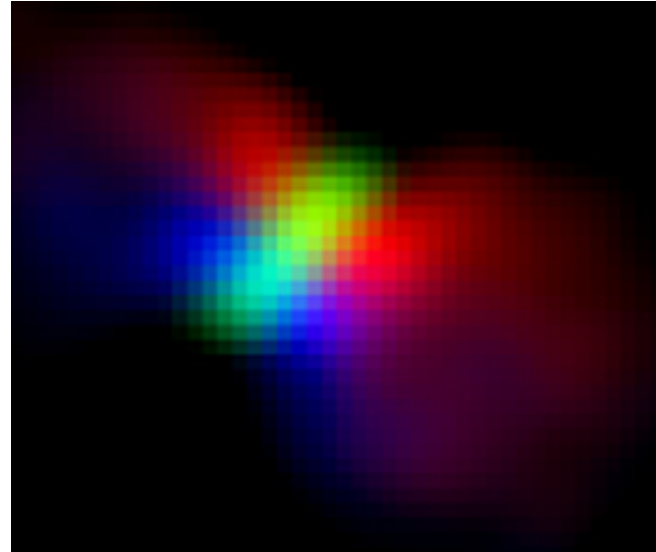
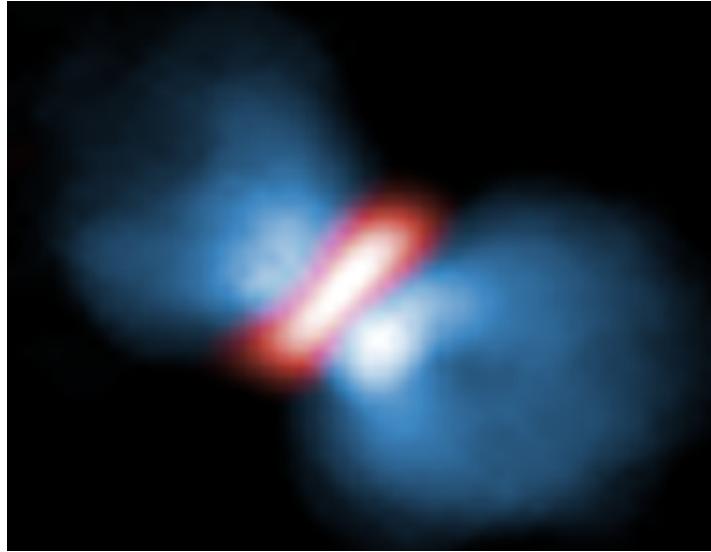
- Introduction - observations, theory
- Numerical simulations in HD and MHD
- “Atlas” of solutions
- Trends in angular momentum flux
- Asymmetry in the accretion funnel
- 3D model from 2D numerical simulations
- Summary

Introduction-observations



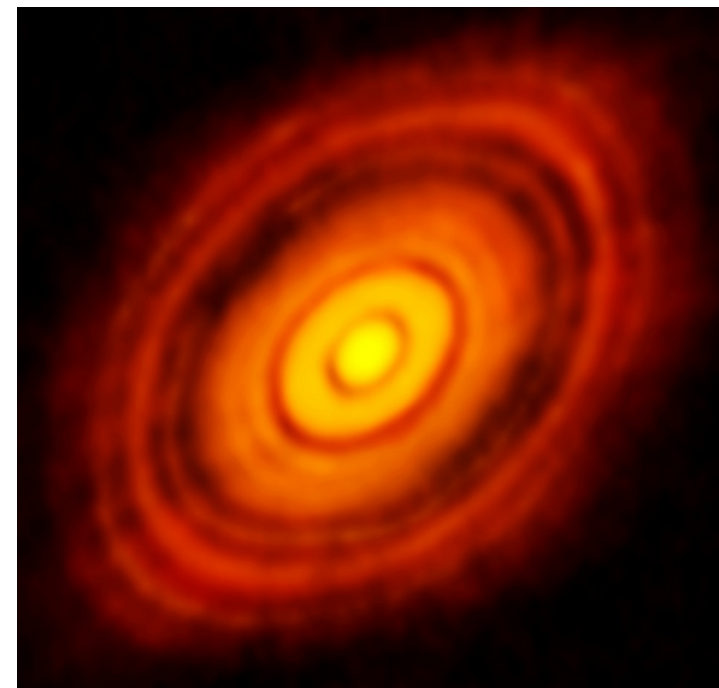
•Stellar jets followed in HH objects in 1950's. Here also only HST provided well resolved disk and jet observations. In the ALMA era, we got even closer-a team from ASIAA, Taiwan recently measured a rotating disk and jet in HH212. Resolution of the observation is down to 8 AU! The angular momentum carried by a jet is so small that it must be launched from the region well inside the disk, about 0.05 AU from the star. This matches with the magnetospheric jet launching.

Introduction-observations



•Stellar outflows in the case of massive young stars comply more to the magnetocentrifugal outflow launching, where the outflow is launched from the disk surface. Here is a recent ALMA image for Orion KL Source 1, and measured velocities. In the right panel the color shows the motion of the gas: red shows gas moving away from us, blue shows gas moving toward us. The disk is shown in green (Hirota et al., 2017).

•Spectacular ALMA image of the HL Tau protoplanetary disk, with the planet trajectories carved-out, is another example of what we can expect from the new instruments (ALMA, 2014). A million years young star with a disk of more than three Neptune orbits radius, is located at 450 ly from us. It came as a large surprise that such a young star would already show signs of planet formation.



Introduction-theory

- First numerical solution of (HD) accretion disk was by Prendergast & Burbidge (1968)
- Analytical solution was given by Shakura & Sunyaev (1973)
- From that time to the 1990-ies many developments and models, with different approximations.
- In Kluźniak & Kita (2000, KK00) was given a solution of the HD disk in the full 3D. It was obtained by the method of asymptotic approximation.
- In 2009, numerical simulations of star-disk magnetospheric interaction were done in 2D-axisymmetric simulations, by Romanova et al. (2009, 2013, with non-public code), Zanni & Ferreira (2009, 2013, with publicly available code).
- Development of disk simulations in the direction of MRI in the disk (Flock et al.), but nothing much in star-disk magnetospheric simulations for a decade.
- In Čemeljić et al. (2017) and Čemeljić (2019), the first repeating of Zanni et al. (2009, 2013) axisymmetric viscous & resistive MHD simulations in 2D with PLUTO code were reported. The results are similar to Romanova et al., obtained with their (non-public) code.
- A parameter study is now possible, to investigate the influence of different parameters-the beginning of this is published in Čemeljić (2019).

Equations for star-disk problem

• I perform simulations of thin accretion disk, which reach a quasi-stationary state.

• Ohmic and viscous heating in the energy equation are neglected, assuming that all the heat is radiated away.

• Viscosity and resistivity are still included, in the equation of motion and in the induction equation.

• Code I use is PLUTO (v.4.1) by Mignone et al. (2007, 2012). Results can be rescaled to different objects:

$$\frac{\partial \rho}{\partial t} + \nabla \cdot (\rho \mathbf{u}) = 0$$

$$\frac{\partial \rho \mathbf{u}}{\partial t} + \nabla \cdot \left[\rho \mathbf{u} \mathbf{u} + \left(P + \frac{\mathbf{B} \cdot \mathbf{B}}{8\pi} \right) \mathbf{I} - \frac{\mathbf{B} \mathbf{B}}{4\pi} - \boldsymbol{\tau} \right] = \rho \mathbf{g}$$

$$\frac{\partial E}{\partial t} + \nabla \cdot \left[\left(E + P + \frac{\mathbf{B} \cdot \mathbf{B}}{8\pi} \right) \mathbf{u} - \frac{(\mathbf{u} \cdot \mathbf{B}) \mathbf{B}}{4\pi} \right] + \nabla \cdot [\eta_m \mathbf{J} \times \mathbf{B} / 4\pi - \mathbf{u} \cdot \boldsymbol{\tau}] = \rho \mathbf{g} \cdot \mathbf{u} - \Lambda_{\text{cool}}$$

$$\frac{\partial \mathbf{B}}{\partial t} + \nabla \times (\mathbf{B} \times \mathbf{u} + \eta_m \mathbf{J}) = 0.$$

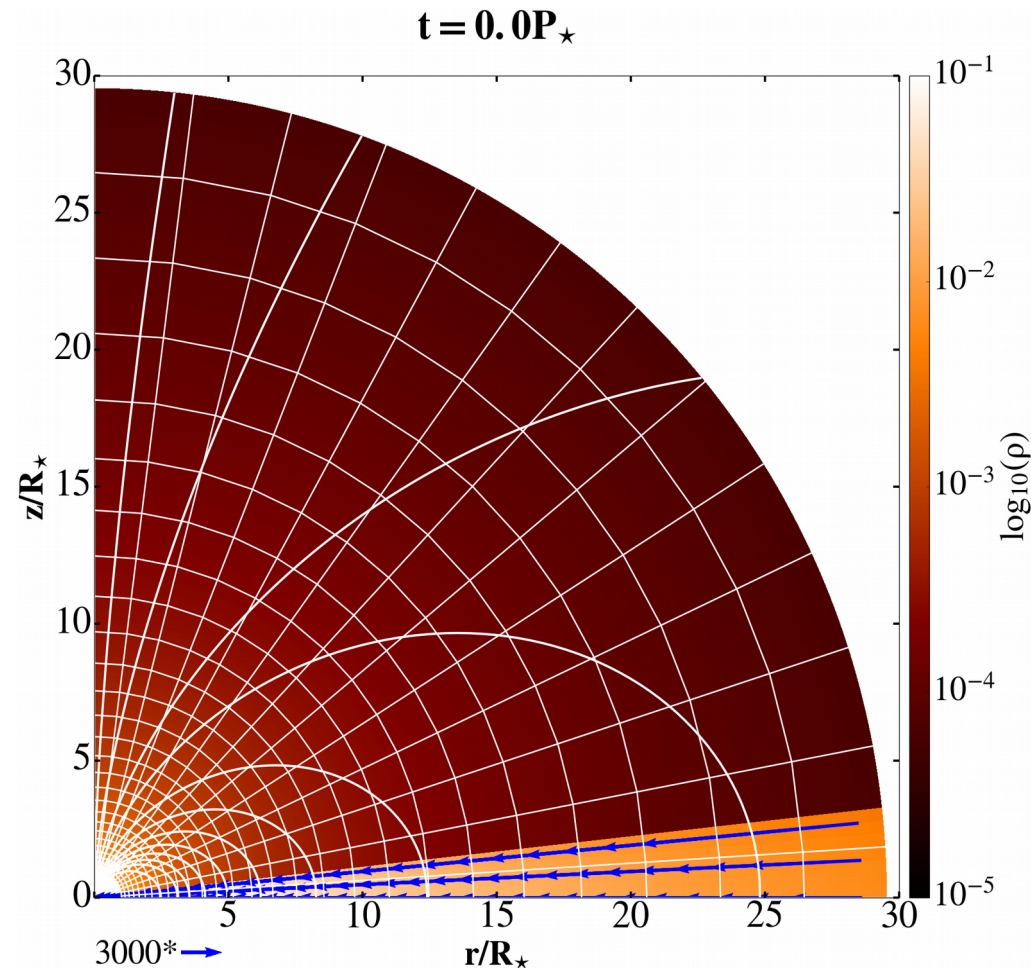
Table A.1. Typical values and scaling for different central objects.

	YSOs	WDs	NSs
$M_{\star} (M_{\odot})$	0.5	1	1.4
R_{\star}	$2R_{\odot}$	5000 km	10 km
P_{\star}	4.6 d	6.1 s	0.46 ms
B_{\star} (G)	500	5×10^5	10^8
$\rho_{\text{d}0}$ (g cm^{-3})	1.2×10^{-10}	9.4×10^{-9}	4.6×10^{-6}
v_0 (km s^{-1})	218	5150	136 000
$\dot{M}_0 (M_{\odot} \text{ yr}^{-1})$	5.7×10^{-7}	1.9×10^{-9}	10^{-9}
B_0 (G)	200	5×10^4	2.93×10^7

Notes. The mass M_{\star} , radius R_{\star} , period P_{\star} and equatorial stellar magnetic field B_{\star} are chosen to derive the rest of the quantities. The code units should be multiplied by the factors given in the table to apply them to different cases.

Star-disk simulations setup

- I add the stellar dipole field to the KK00 solution. Simulations with quadrupole, octupole and multipole field were also performed.
- Stellar surface is a rotating boundary around the origin of the spherical computational domain. We assume the star to be a (differentially) rotating magnetized rotator—we correct for the azimuthal component of the torque atop the star.
- The initial corona is a non-rotating corona in a hydrostatic balance.

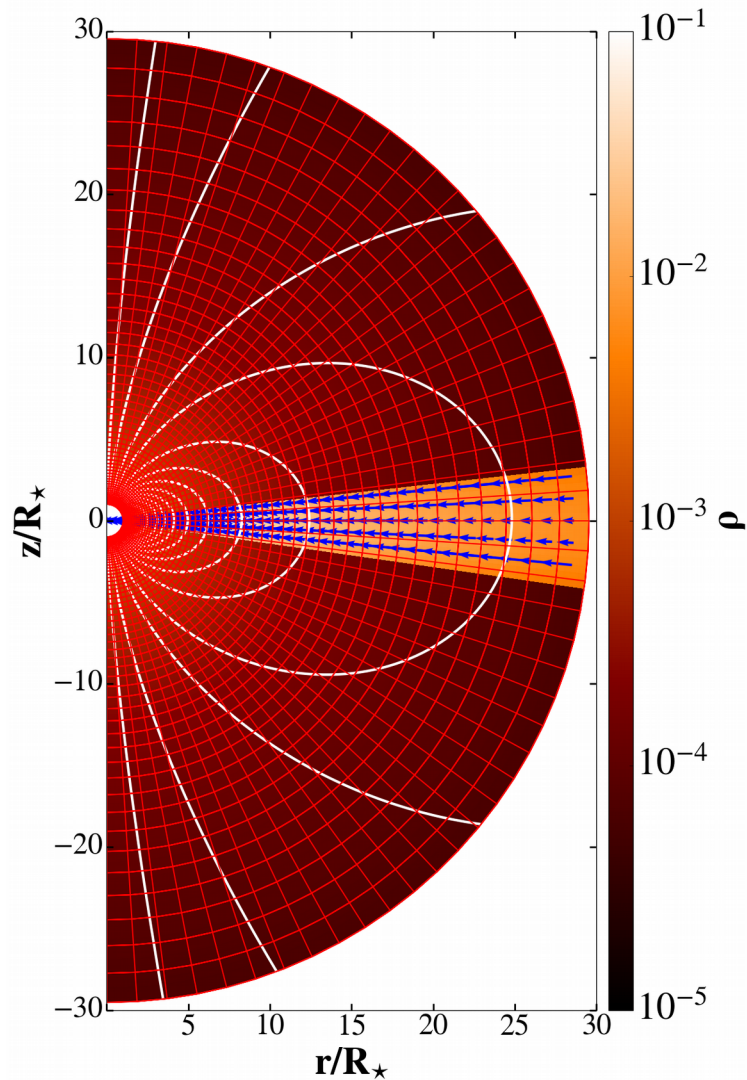


- In Čemeljić (2019) I performed a systematic study with magnetic star-disk numerical simulations, in 64 points in parameter space, for slow rotating star (up to 20% of the breakup velocity of the star). Cases with faster rotating star are currently investigated in work with A. Kotek.

The asymmetric jet launching (with A. Kotek)

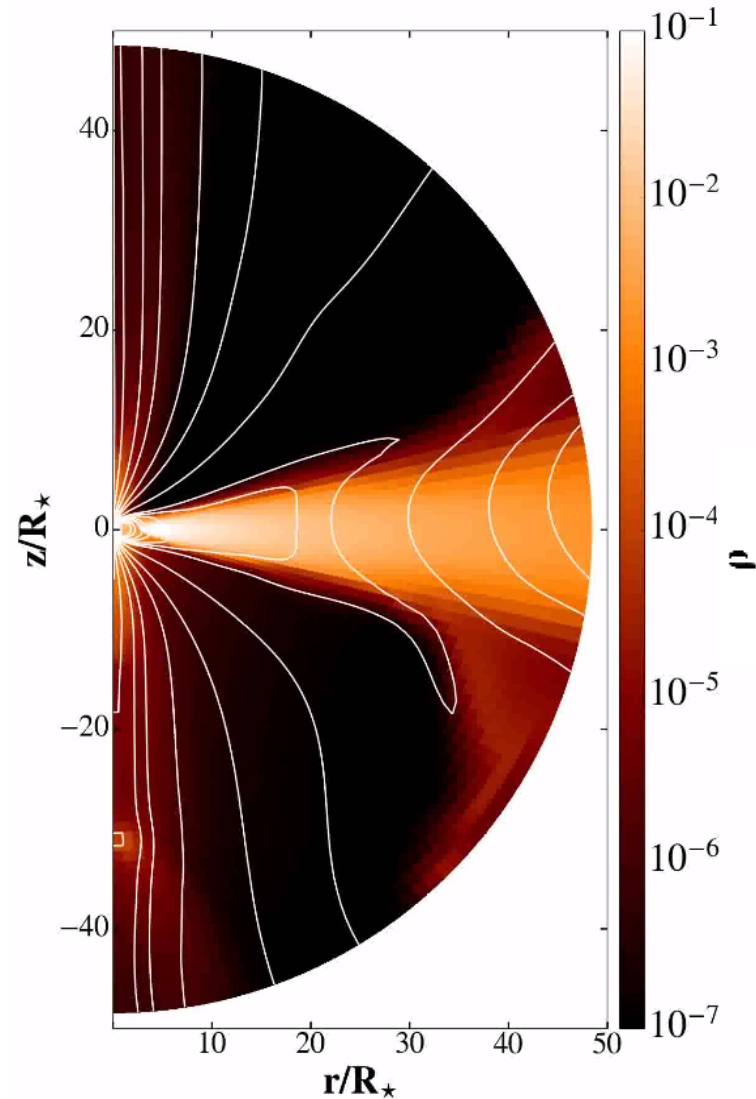
With A. Kotek we took another look at the solutions with the jet launching: in the full meridional plane, with $R \times \vartheta = [217 \times 200]$ grid cells in $\vartheta = [0, \pi]$. We obtain and analyze the asymmetric jets launched from the star-disk magnetosphere.

$t = 0.0 P_{\star}$



Initial setup in a full meridional plane.

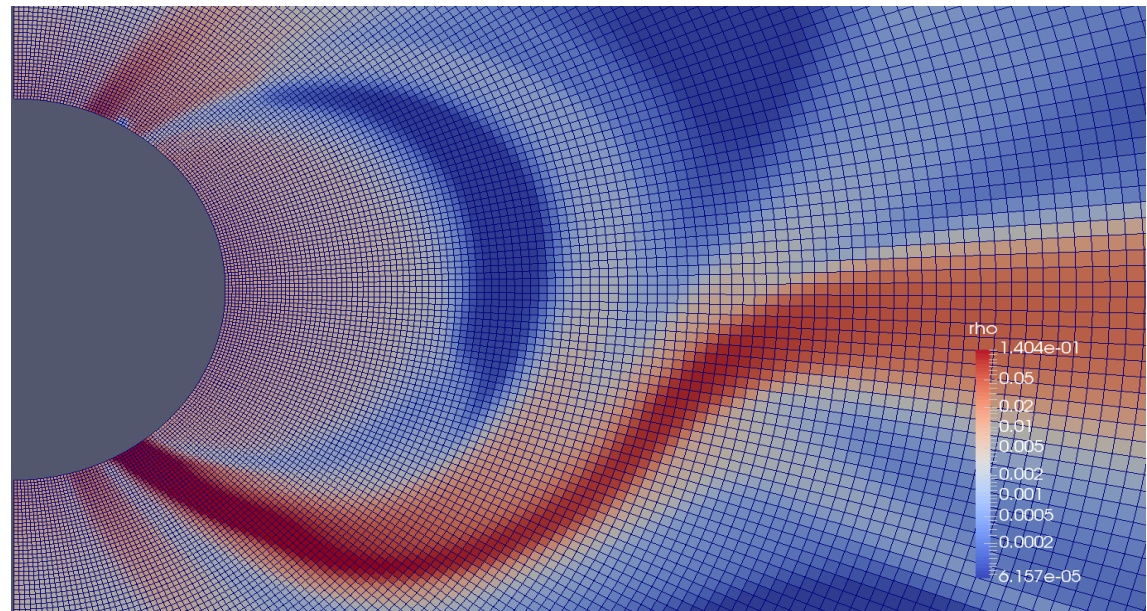
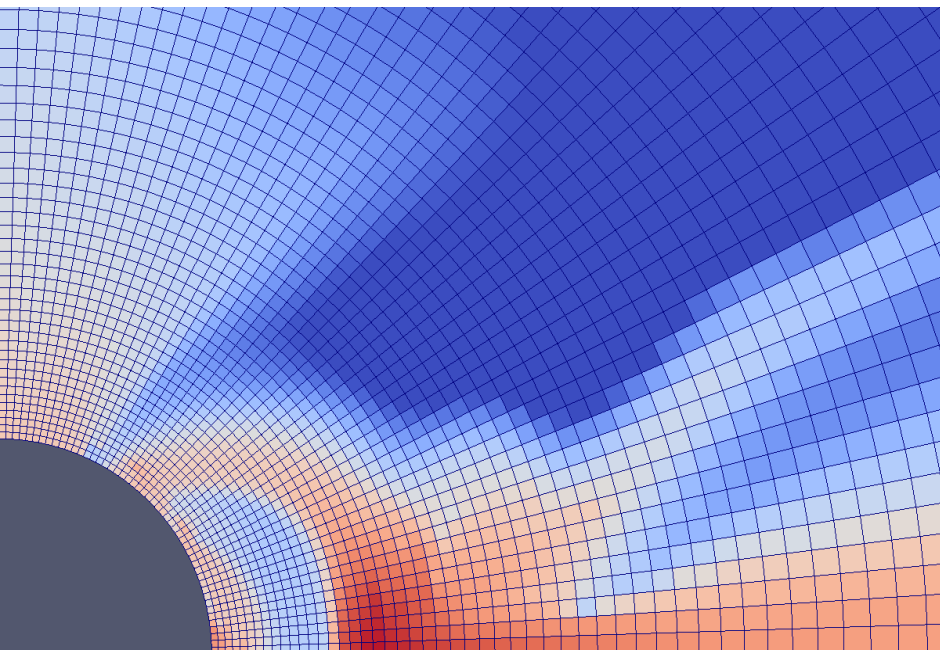
$t = 60.0 P_{\star}$



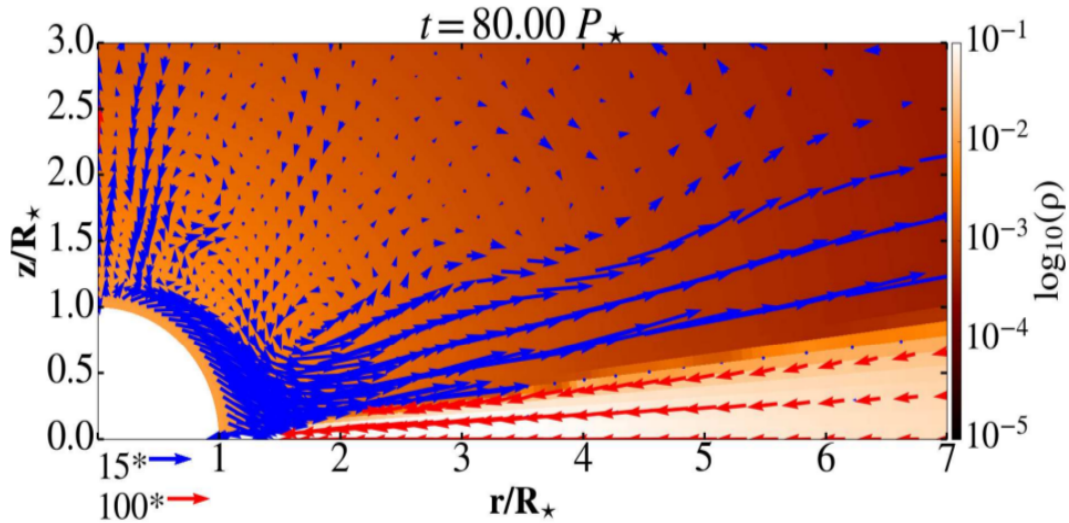
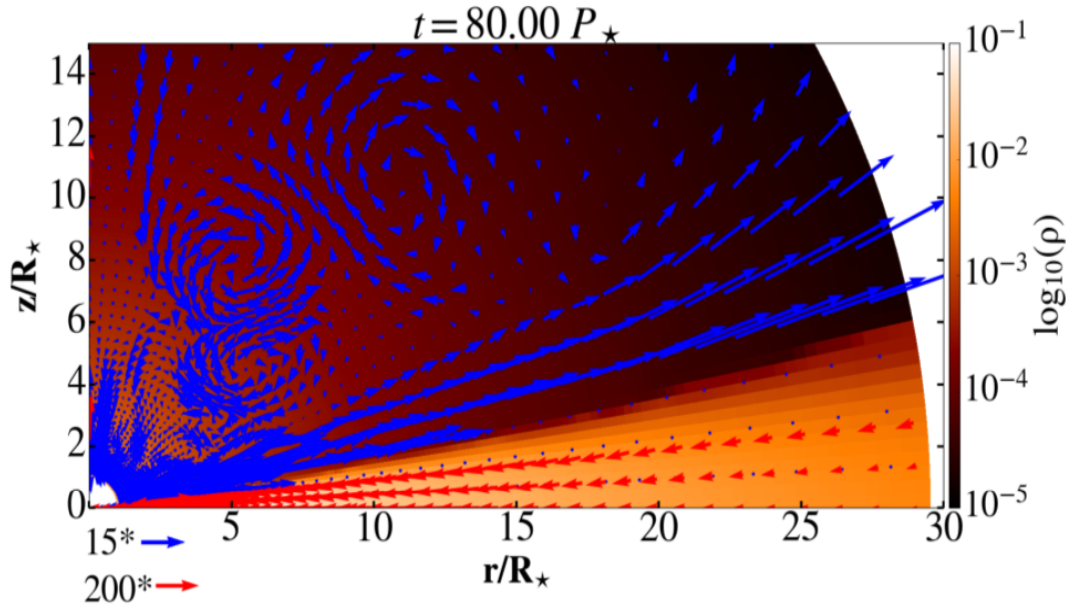
Asymmetric jet launched from the magnetosphere.

Star-disk simulations setup

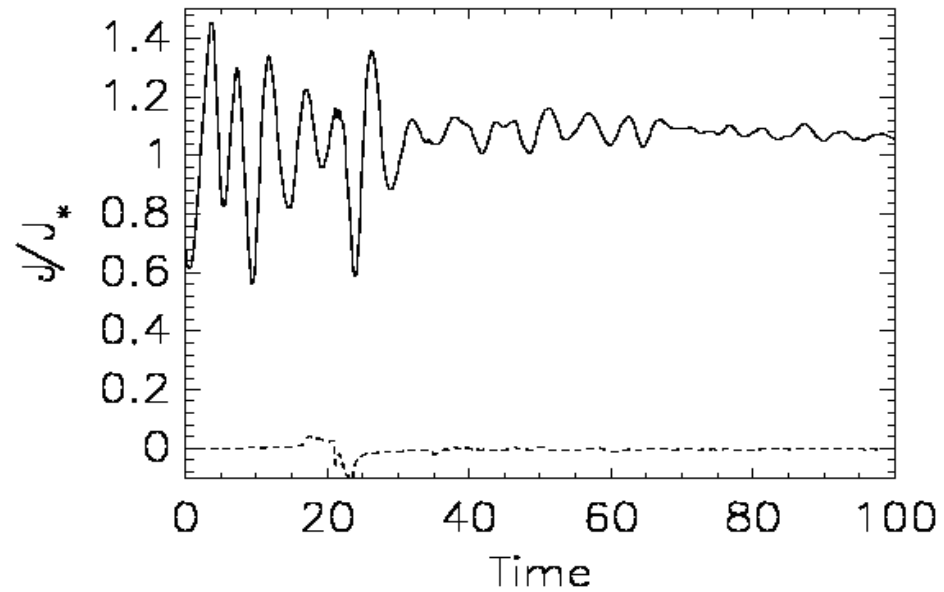
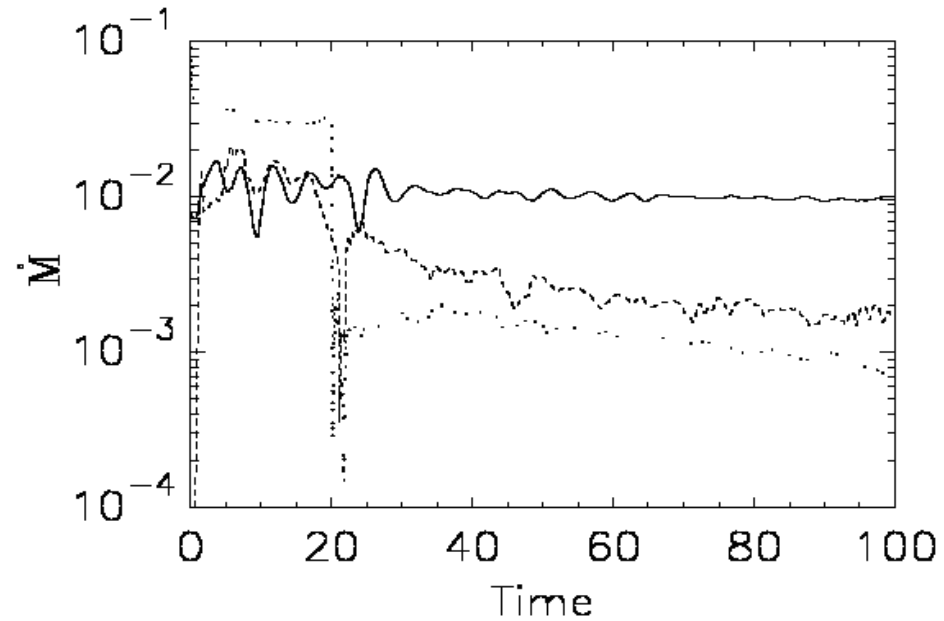
- Resolution is $R \times \vartheta = [217 \times 100]$ grid cells in $\vartheta = [0, \pi/2]$, with a logarithmic grid spacing in the radial direction. The accretion column is well resolved.
- Star rotates at about 1/10 of the breakup rotational velocity.
- I did also $R \times \vartheta = [217 \times 200]$ grid cells in $\vartheta = [0, \pi]$ – no disk equatorial B.C.



Hydro-dynamical star-disk simulations

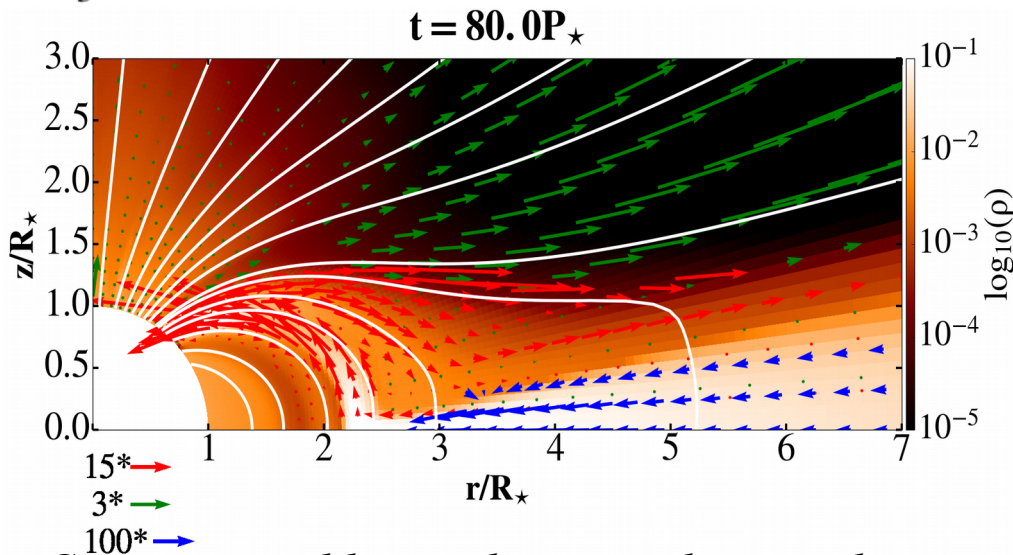
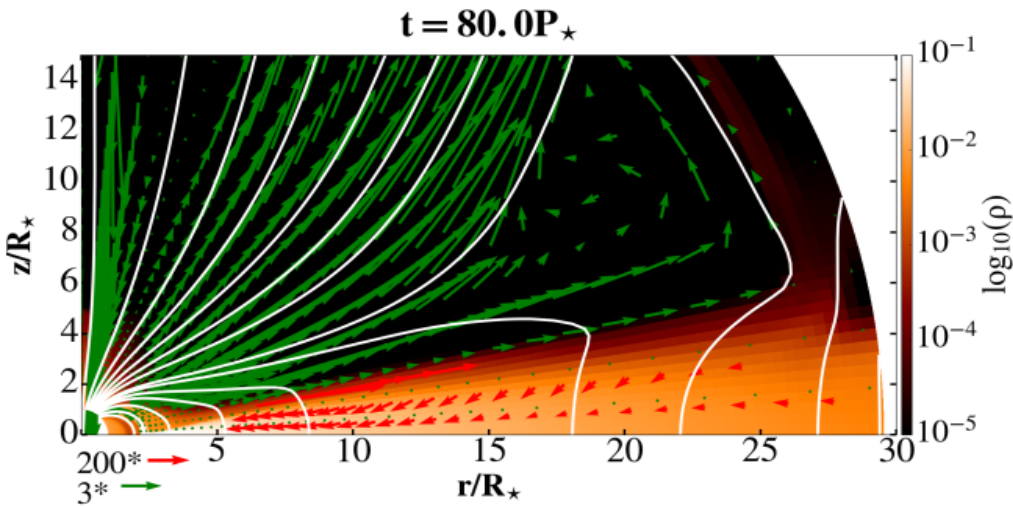


Computational box and a zoom closer to the star after 80 stellar rotations. In color is shown the density, and vectors show velocity, with the different normalization in the disk and stellar wind.

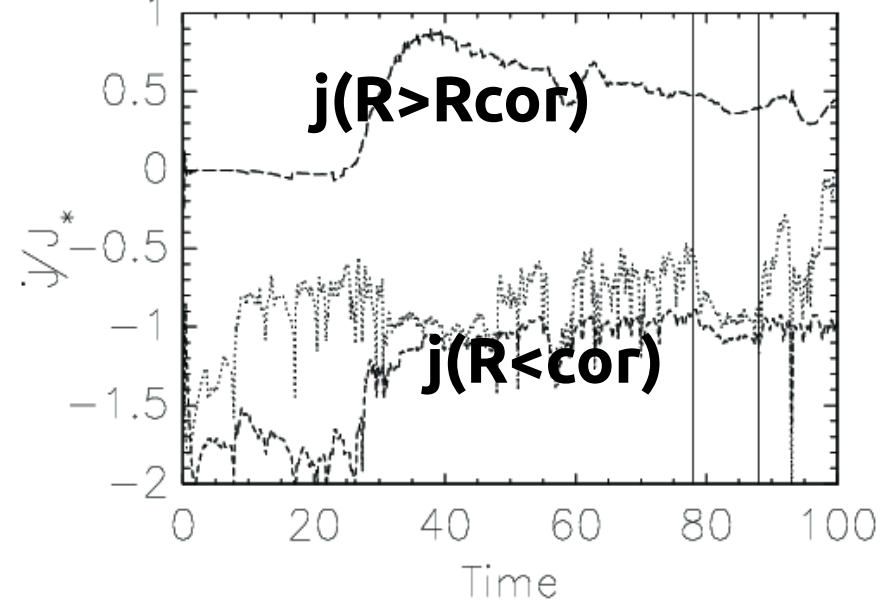
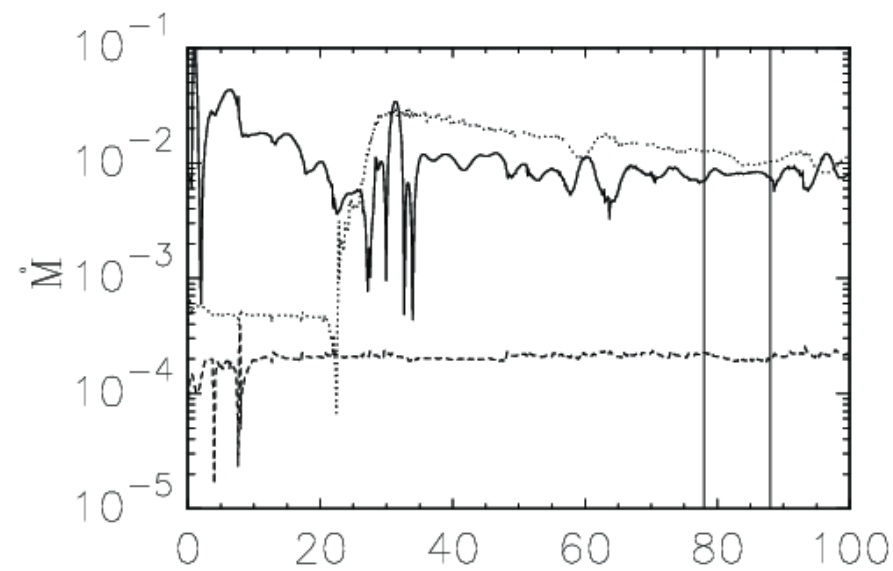


Time dependence of the mass and angular momentum fluxes in the various components in our simulations.

Star-disk magnetospheric interaction (SDMI) simulations

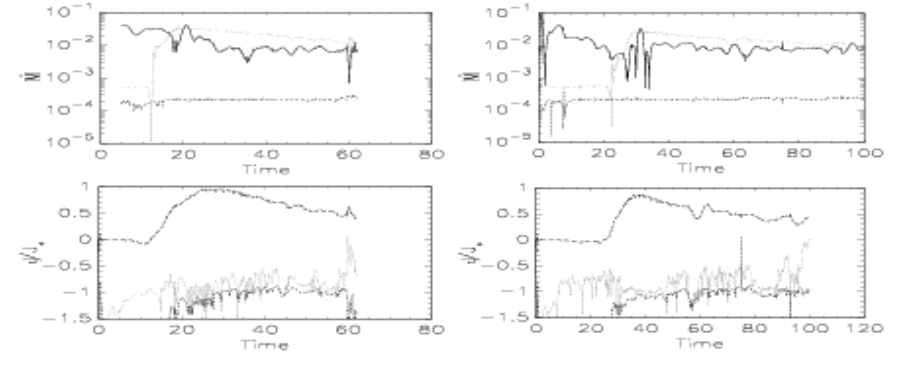
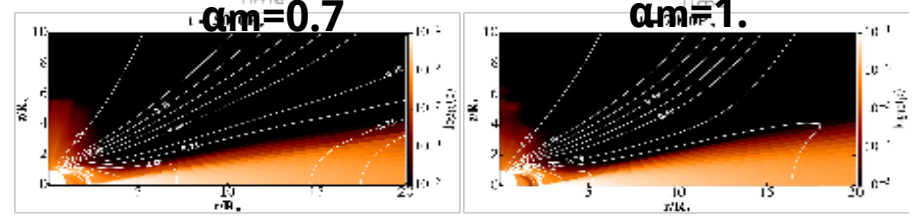
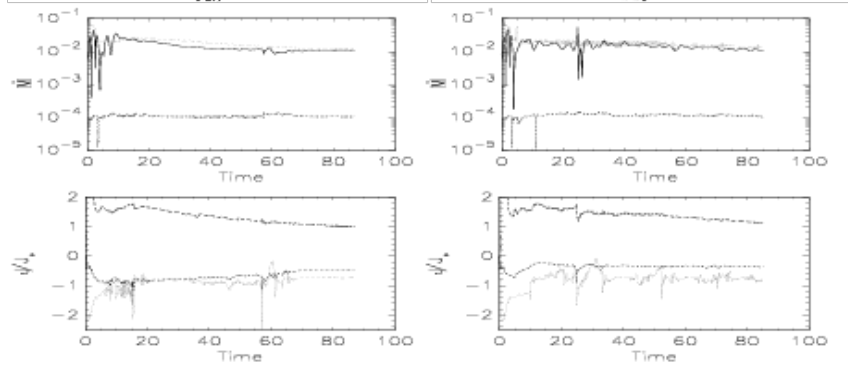
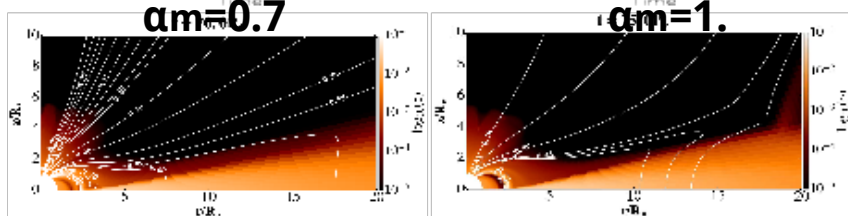
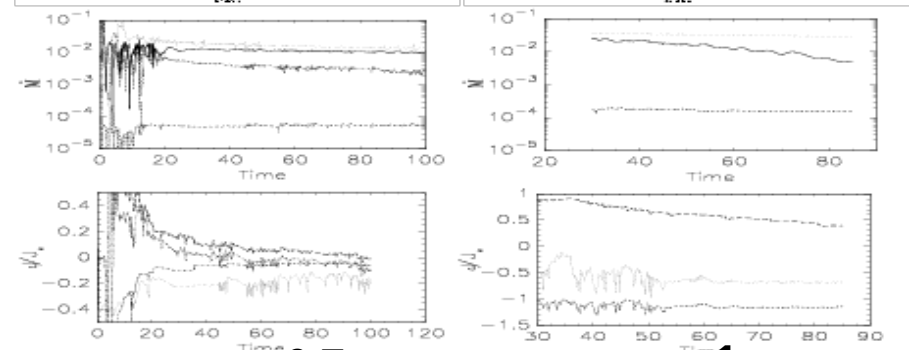
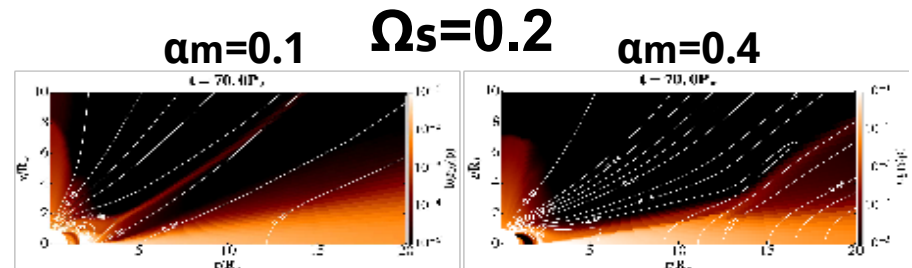
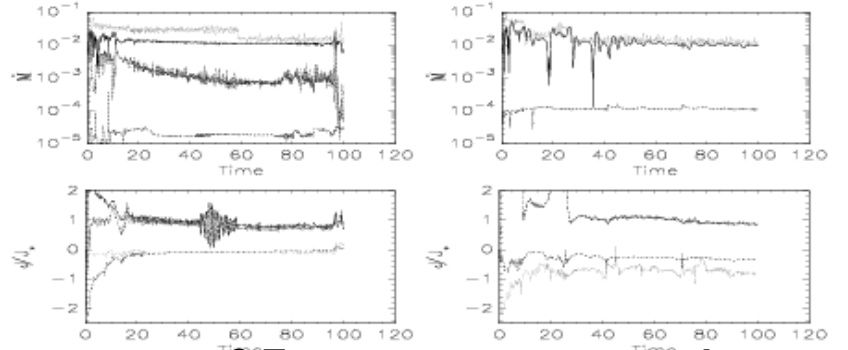
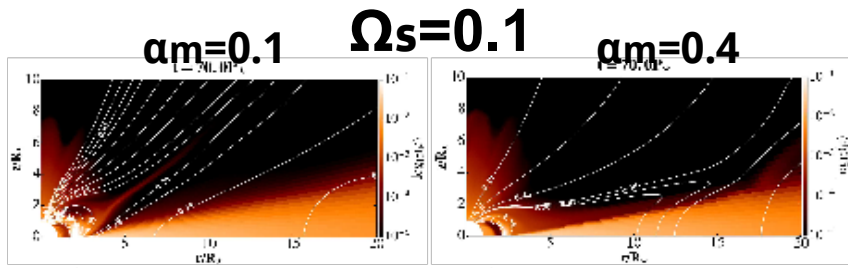


Computational box and a zoom closer to the star after 80 stellar rotations, to visualize the accretion column and the magnetic field lines (white solid lines) connected to the disk beyond the corotation radius $R_{\text{cor}} = 2.92 R_{\text{s}}$. In color is shown the density, and vectors show velocity, with the different normalization in the disk, column and stellar wind.

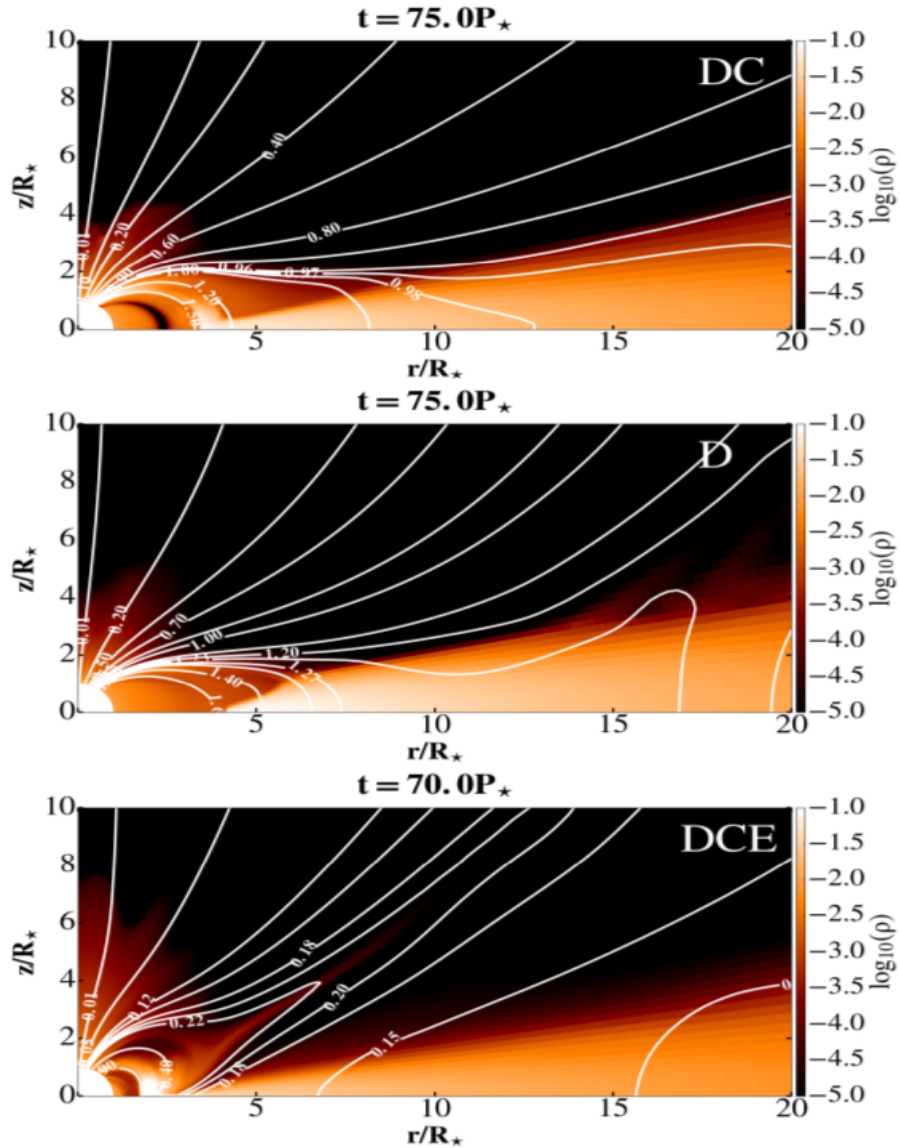


Time dependence of the mass and angular momentum fluxes in the various components in our simulations with marked the time interval in which the average for the quasi-stationarity is computed.

Part of the “Atlas” of solutions with different resistivities



Configurations in “Atlas” solutions for slowly rotating stars



Three different cases of geometry in the results. In the top and middle panels are shown $B=1$ kG and the resistivity $\alpha_m=1$, in the cases with $\Omega_s=0.1$ (top panel) and $\Omega_s=0.15$ (middle panel). Faster stellar rotation prevents the accretion column formation. In the bottom panel is shown the third case, with $B=0.5$ kG, resistivity $\alpha_m=0.1$ and $\Omega_s=0.1$, where a conical outflow is formed.

$\alpha_m =$	0.1	0.4	0.7	1
Ω_*/Ω_{br}				
$B_* = 250$ G				
0.05	DCE	DC	DC	DC
0.1	DCE	DC	DC	DC
0.15	DCE	DC	DC	DC
0.2	DCE	DC	DC	DC
$B_* = 500$ G				
0.05	DCE	DC	DC	DC
0.1	DCE	DC	DC	DC
0.15	DCE	DC	DC	DC
0.2	DCE	DC	DC	DC
$B_* = 750$ G				
0.05	DCE	DC	DC	DC
0.1	DCE	DC	DC	DC
0.15	DCE	DC	DC	DC
0.2	DCE	DC	DC	DC
$B_* = 1000$ G				
0.05	DCE	DC	DC	DC
0.1	DCE	DC	DC	DC
0.15	DCE	D	D	D
0.2	DCE	D	D	D

“Atlas” results: trends

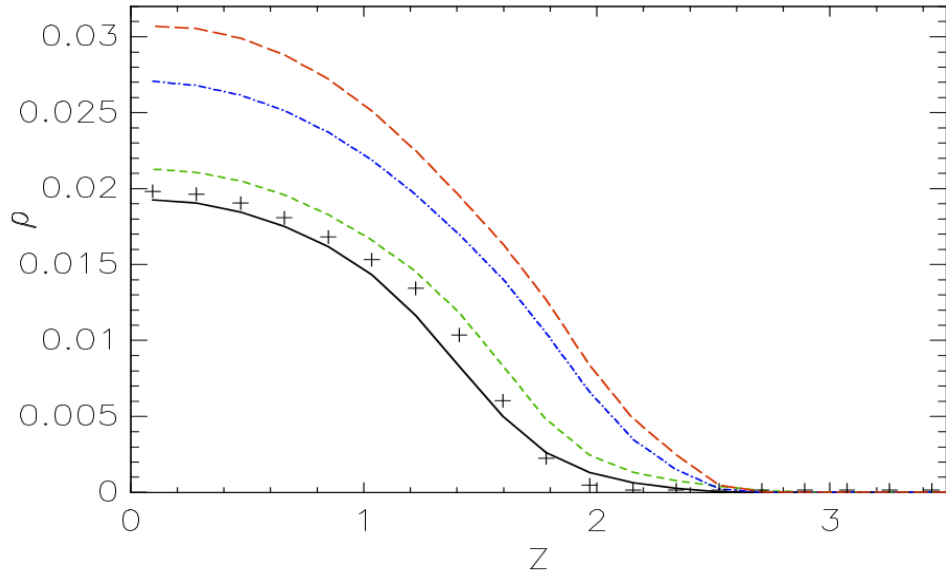


Fig. 3. Disk density in the simulations with $\Omega_\star = 0.2\Omega_{\text{br}}$ and $\alpha_m = 1$, measured along the disk height at $R = 12R_\star$. Results for $B_\star = 0.25$ (solid black line), 0.5 (short dashed green line), 0.75 (dash-dotted blue line) and 1 kG (long dashed red line) are shown. There is a trend in density with increasing stellar field. The result in the simulations without a magnetic field is shown with pluses.

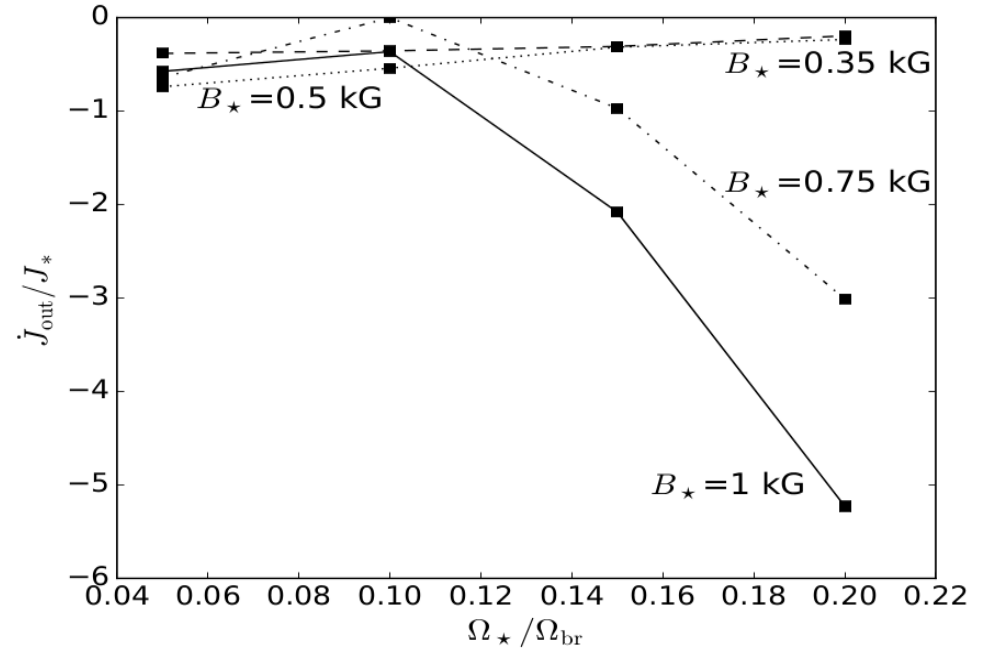


Fig. 5. Average angular momentum flux in the outflow that forms for $\alpha_m = 0.1$. It is computed at $R = 12R_\star$ for different stellar rotation rates. Normalization is the same as in Fig. 4. Fluxes in $B_\star = 0.25$ (dotted), 0.5 (dash-dotted), 0.75 (dashed) and 1 kG (solid) are shown.

“Atlas” results: trends

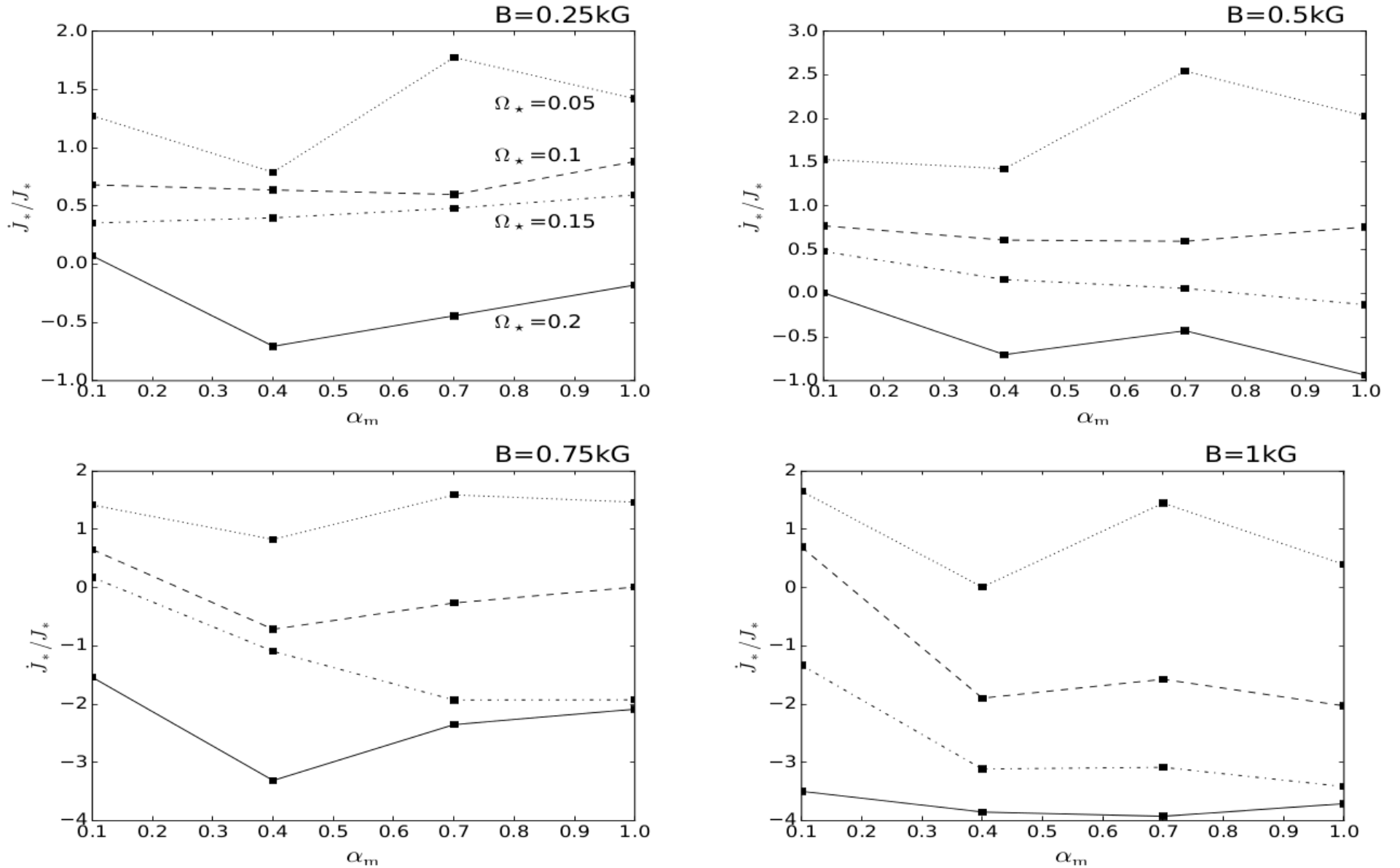
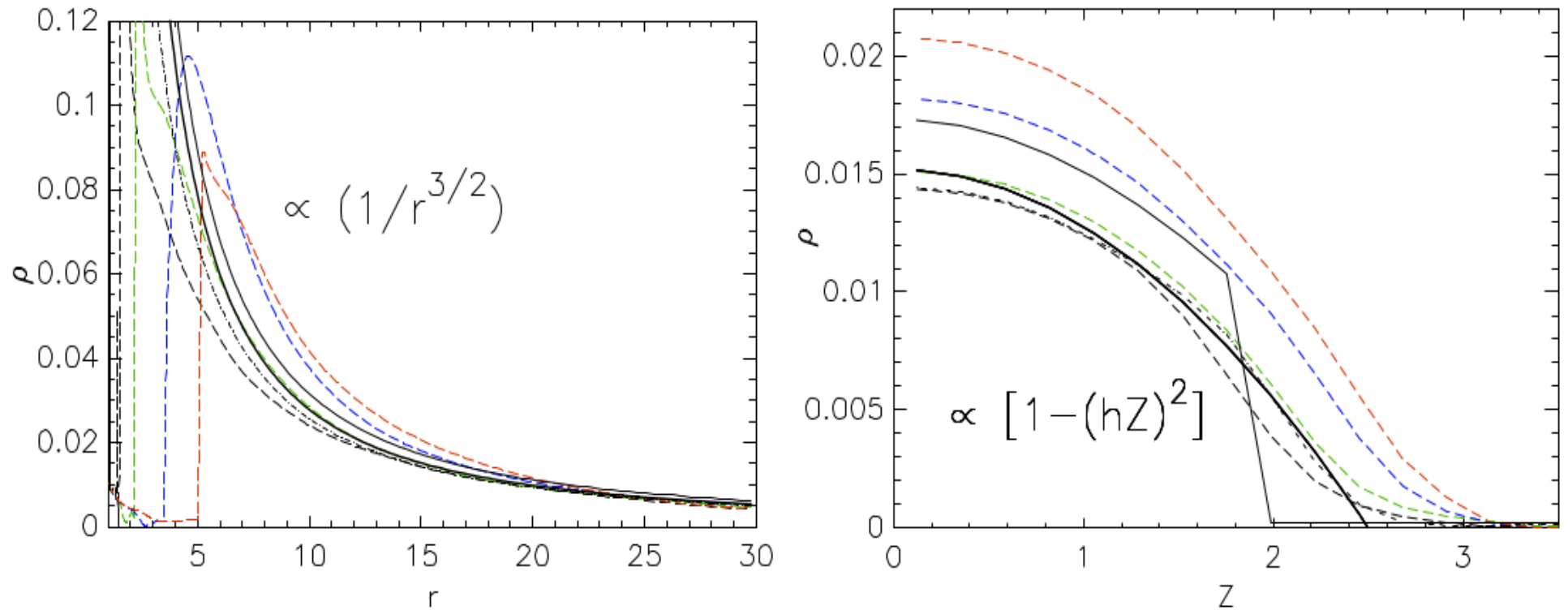


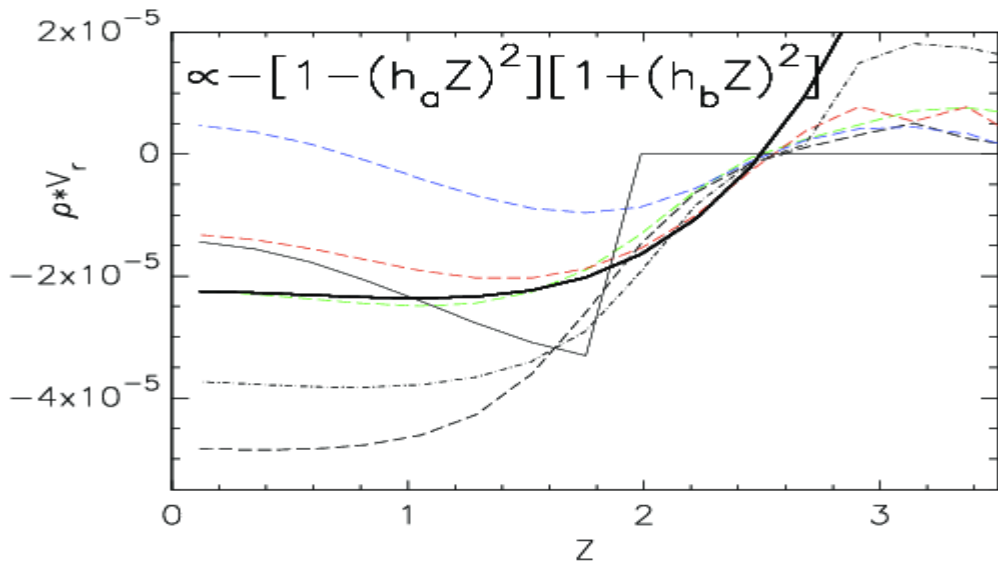
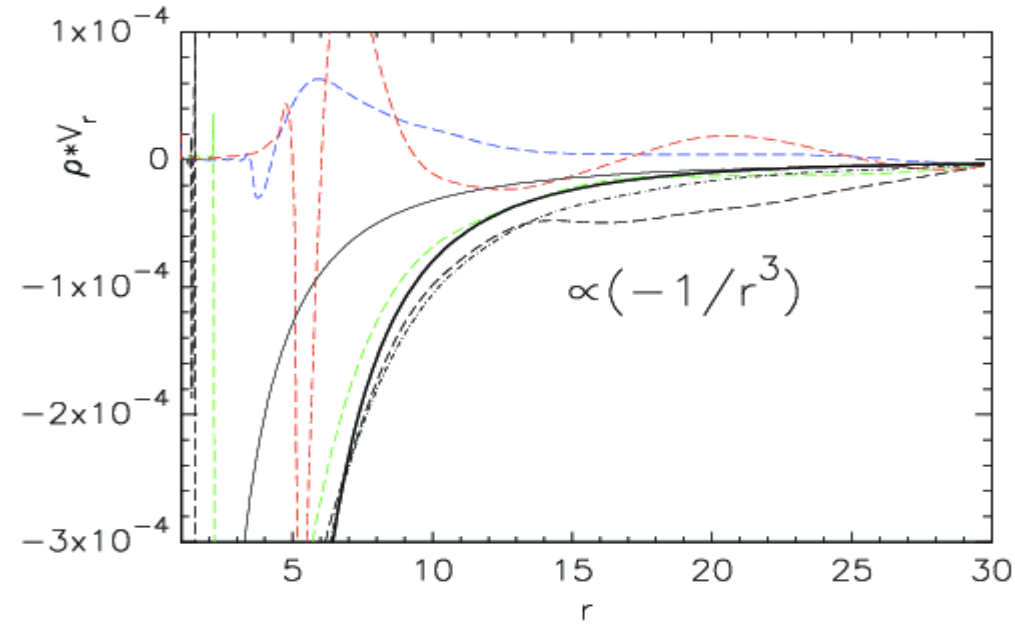
Fig. 4. Average angular momentum flux transported onto the stellar surface by the matter in-falling from the disk onto the star through the accretion column. Each panel shows a set of solutions with one stellar magnetic field strength and varying stellar rotation rate and resistivity. Results with $\Omega_\star / \Omega_{\text{br}} = 0.05$ (dotted), 0.1 (dashed), 0.15 (dash-dot-dotted), and 0.2 (solid) are shown in units of stellar angular momentum $J_\star = k^2 M_\star R_\star^2 \Omega_\star$ (with $k^2 = 0.2$ for the typical normalized gyration radius of a fully convective star). A positive flux spins the star up, a negative flux slows it down. With the increase in stellar rotation rate, spin-up of the star by the infalling matter decreases and eventually switches to spin-down.

Comparison of results with increasing mag. field



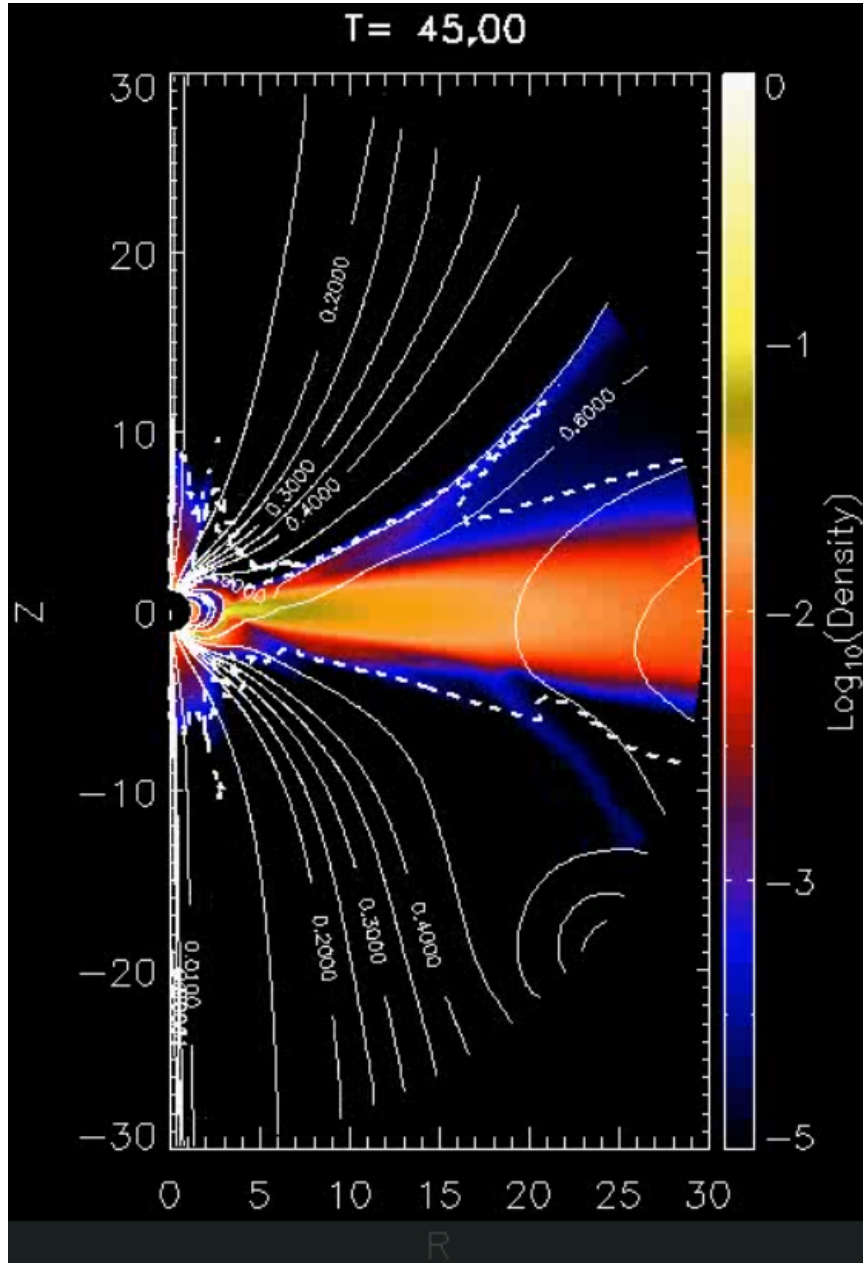
Comparison of the matter density in the initial set-up (thin solid line) with the quasi-stationary solutions in the numerical simulations in the HD (dot-dashed line) and the MHD (long-dashed line) cases. In black, green blue and red colors are the results in the MHD cases with the stellar magnetic field strength 0.25, 0.5, 0.75 and 1.0 kG, respectively. The closest match to the 0.5 kG case is depicted with the thick solid line. In the left panel is shown the radial dependence nearby the disk equatorial plane, and in the right panel the profiles along the vertical line at $r=15$.

Comparison of results with increasing mag. field



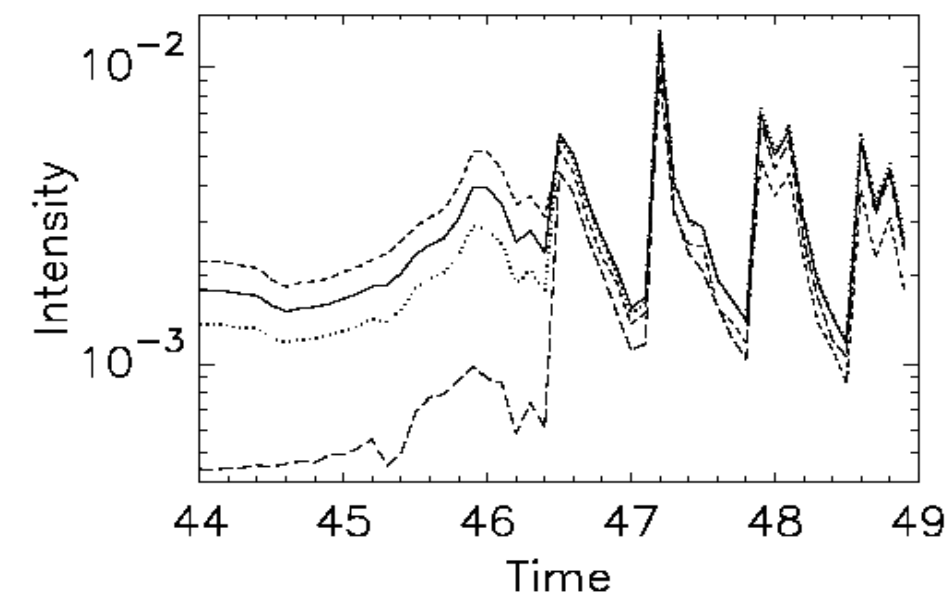
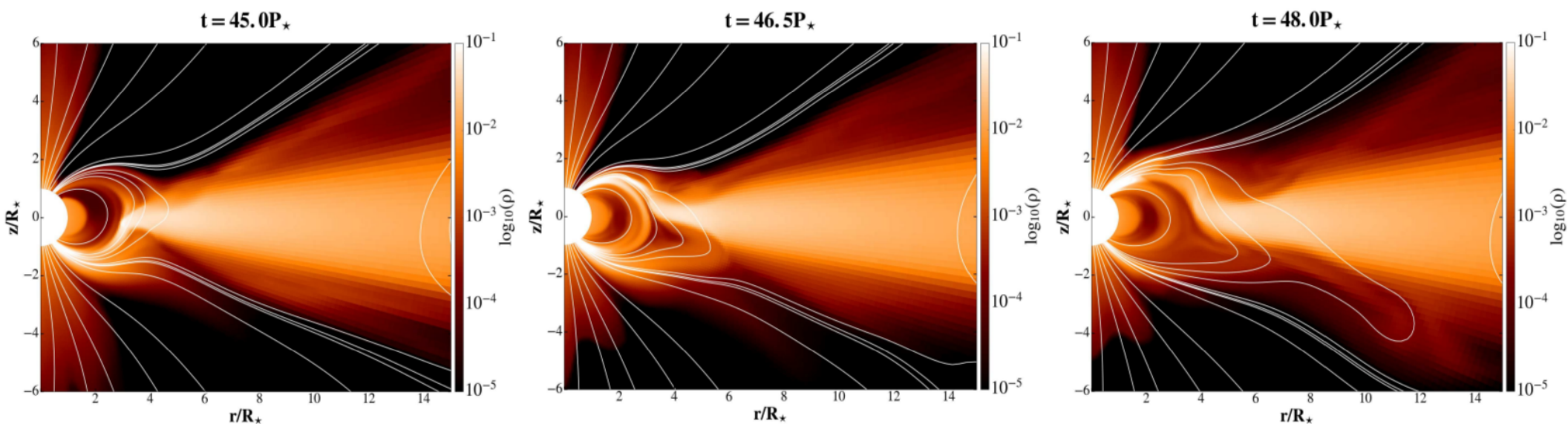
Comparison for the radial momentum. In black, green blue and red colors are the results in the MHD cases with the stellar magnetic field strength 0.25, 0.5, 0.75 and 1.0 kG, respectively. The closest match to the 0.5 kG case is depicted with the thick solid line.

Animation of results with dipole magnetic field



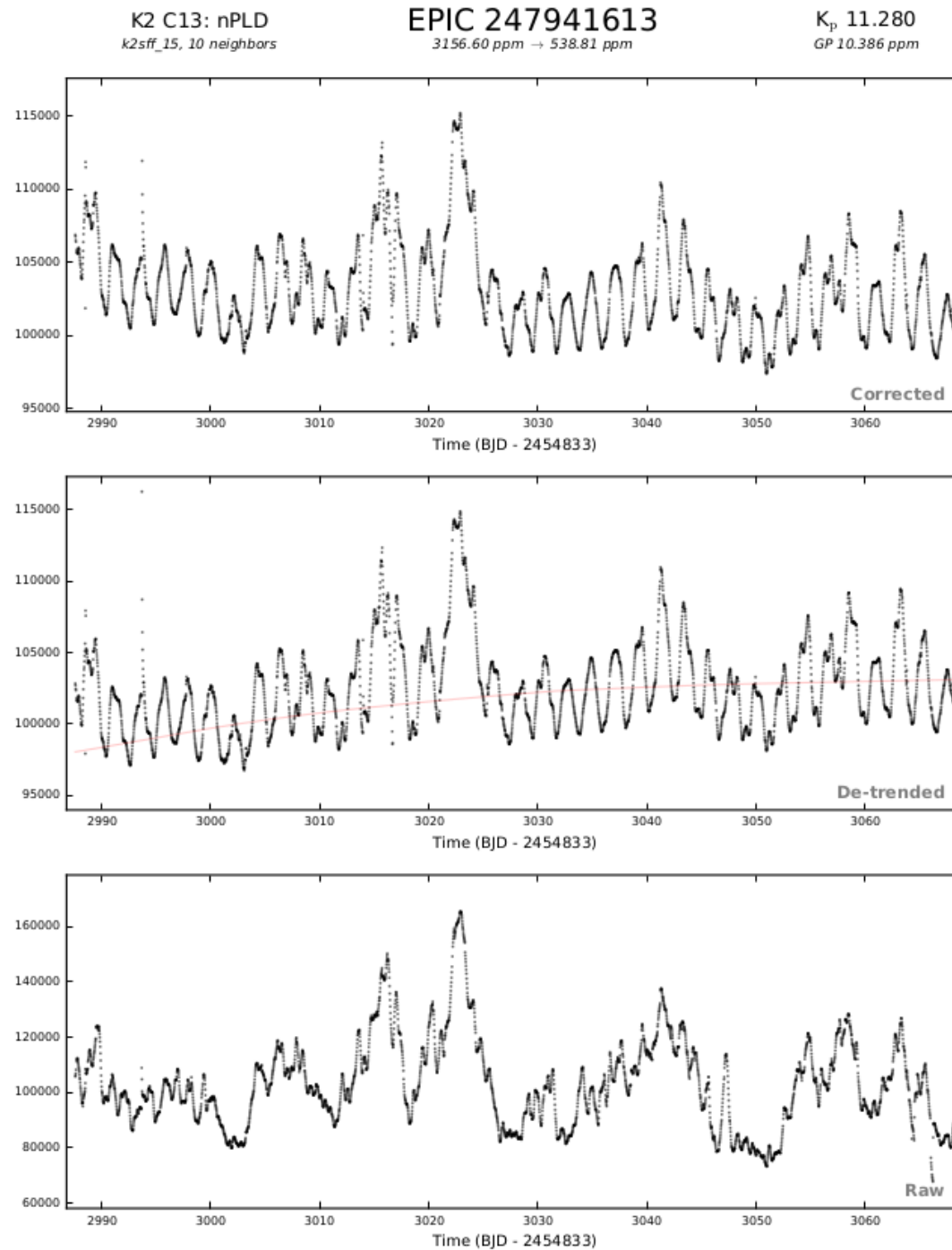
Density in logarithmic color grading, overplot with a sample of magnetic field lines. Accretion column switches position of the attachment to the star-footpoint “jumps” from the southern to northern stellar hemisphere. This happens during the relaxation from the initial and boundary conditions, but also with already relaxed disk. Why?

Bonus: switching mechanism with the magnetic field aligned with the rotation axis



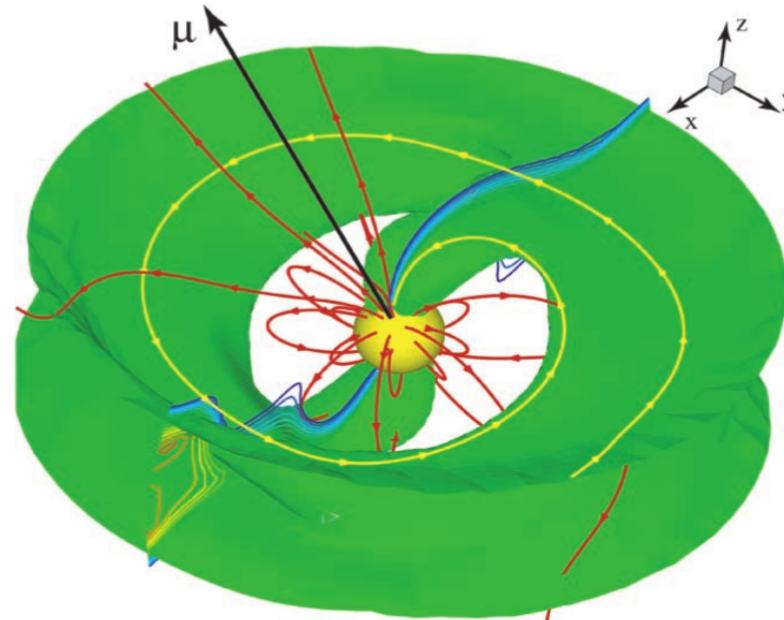
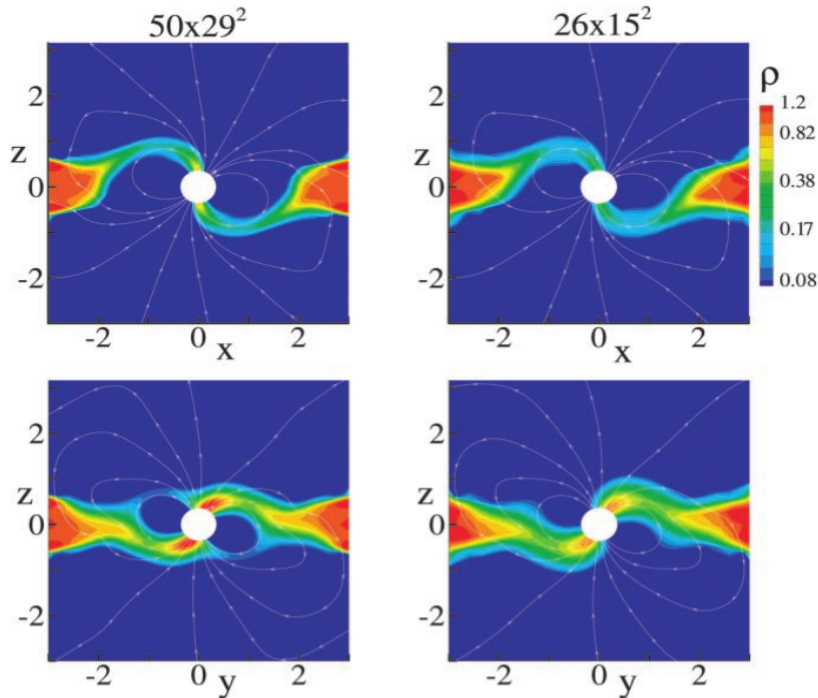
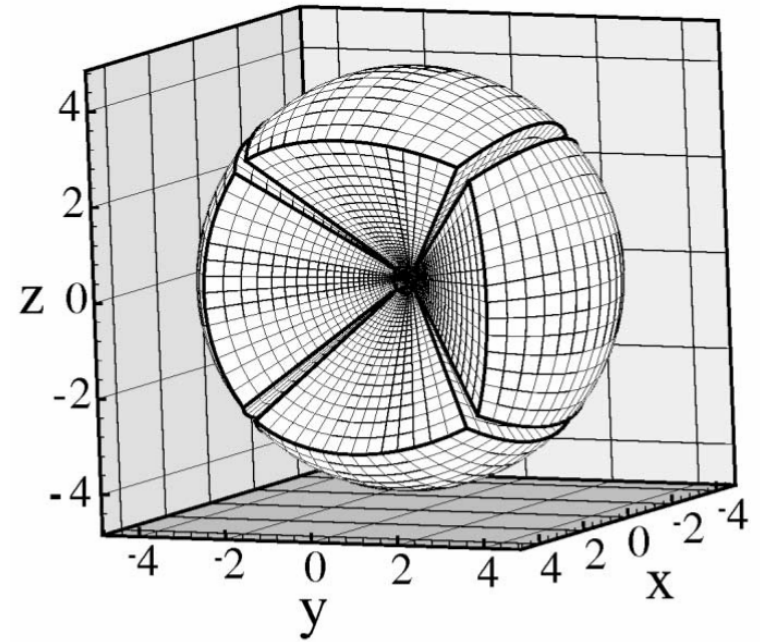
The emission integrated along the stellar rim one grid cell thick in the azimuthal direction. The solid, dotted, long-dashed and short-dashed lines represent the intensities for an observer positioned at a co-latitudinal angle $\theta = 15, 30, 60$ and 165 degrees, respectively.

Observer's input: curious case of V1000 Tau (M. Siwak)



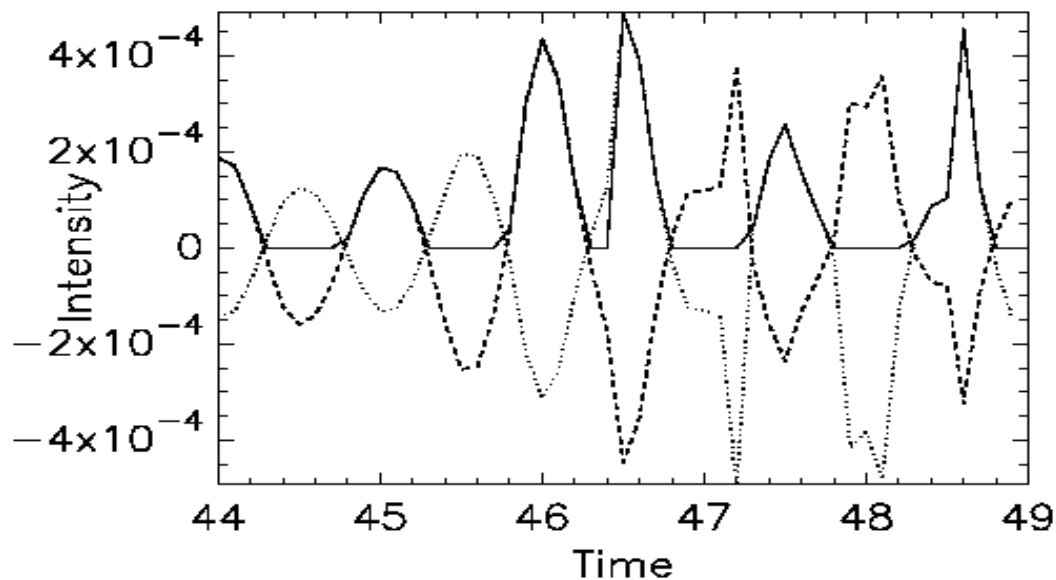
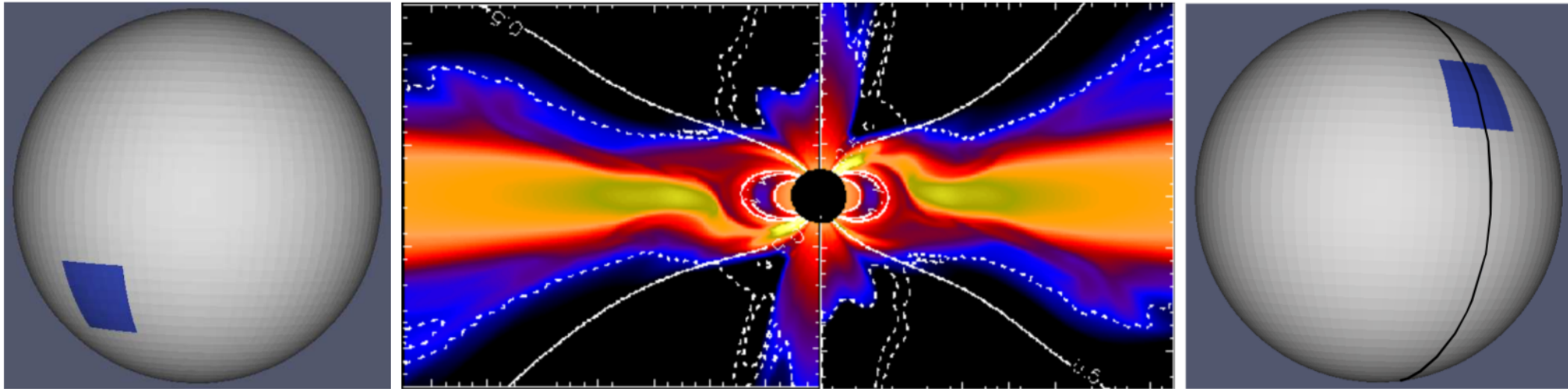
3D results, Romanova et al.

- Ultimate goal of simulations work is to create a simulation which would produce the synthetic maps, which then could be compared with the observations.
- In simulations of magnetospheric star-disk interaction there is currently only one successful setup in 3D: Romanova et al.
- Thanks to A. Koldoba's implementation of "cubed sphere" grid, this group produced, during the last 20 years, beautiful simulations with rotating star, disk and accretion column of matter from the disk onto a star.



Connection of 2D simulations to observations: 2D model for 3D light curve

The 3D simulations are tricky to obtain. Even if one does so, to make a parameter study is not straightforward. To use the 2D simulations with realistic parameters, I constructed a 3D model.



The dotted and dashed lines show the intensity for modeled hot spots as seen from the co-latitude angles of $\theta = 15$ and $\theta = 165$ degrees. Intensity is negative when the spot is not visible from a given position. In solid line is shown the total intensity for an observer with $\theta = 165$. Switching of the accretion column from the southern to northern hemisphere produces a phase shift in the observed intensity peak as the star rotates.

Referee: artificial hot spots not good enough. Wrong.
Model revisited: 2D axisymmetric simulation gives 3D model

New 3D model, made without “inventing” the diametrically opposite hot spot.

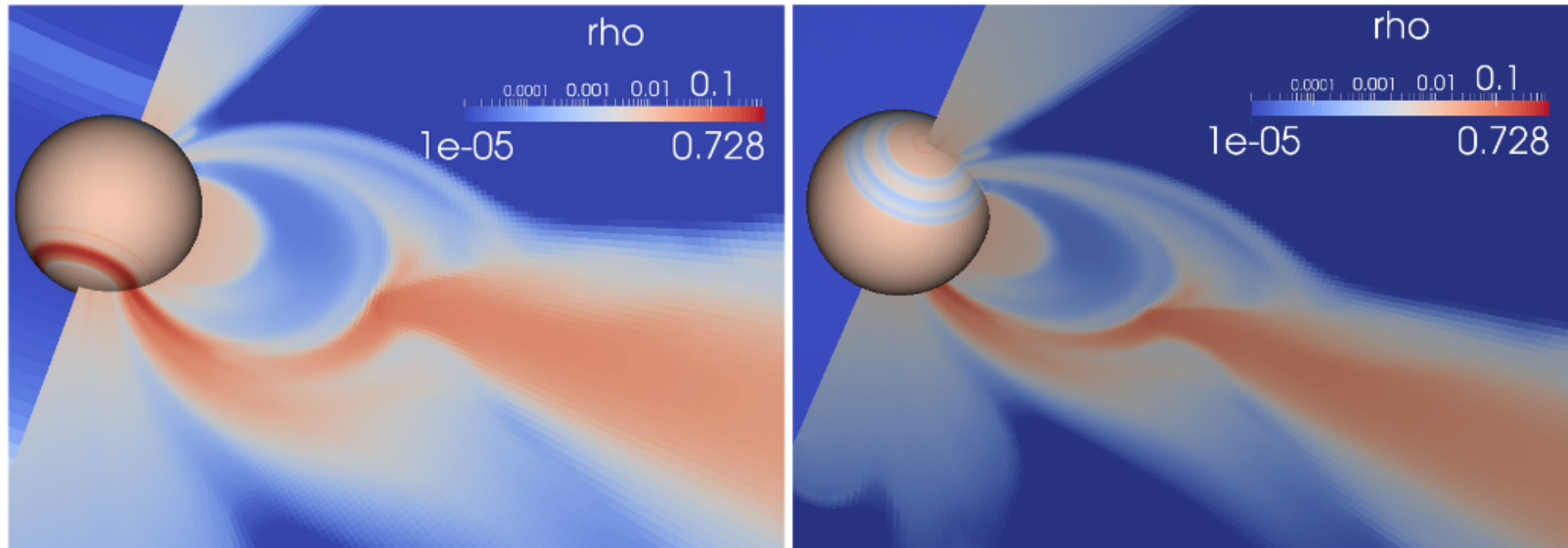


Figure 5. Snapshots in our 3D model from 2D-axisymmetric simulations at $T=45$ stellar rotations, with a cut in the meridional plane to show the accretion column and disk. In the left panel is shown a view to the southern hemisphere, with a ring-shaped hot spot at the foot-points of the accretion column. In the right panel is shown a view to the northern hemisphere, with a less dense ring-shaped hot spot than in the southern hemisphere.

Back to drawing board: Initial switching

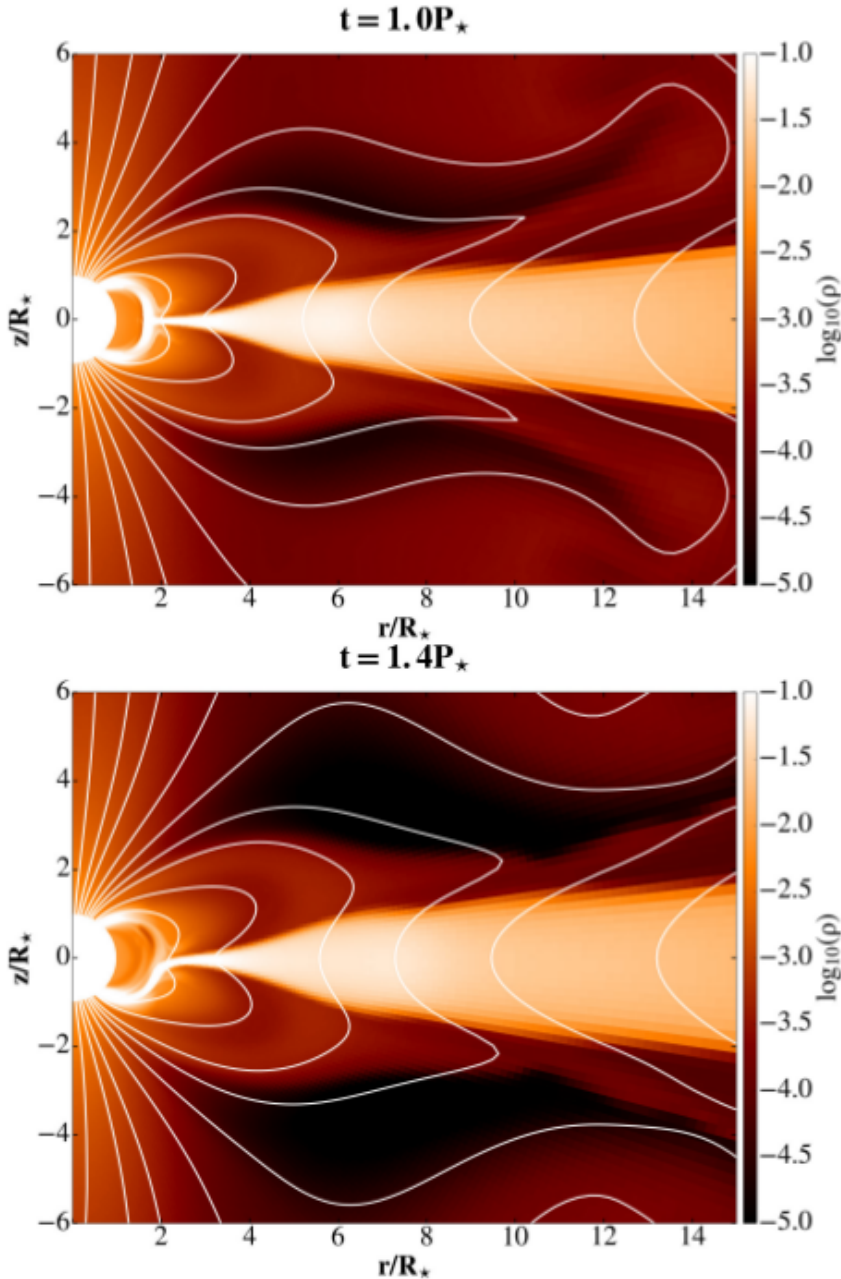


Figure 2. The density in the units of ρ_{d0} and a sample of magnetic field lines in the snapshots in results after $T=1$ and $T=1.4$ stellar rotations. The initially symmetric accretion columns (which are in 2D axisymmetric solution curtains) become asymmetric with respect to the disk equatorial plane before the relaxation from the initial and boundary conditions. The solution remains asymmetric further in the simulation.

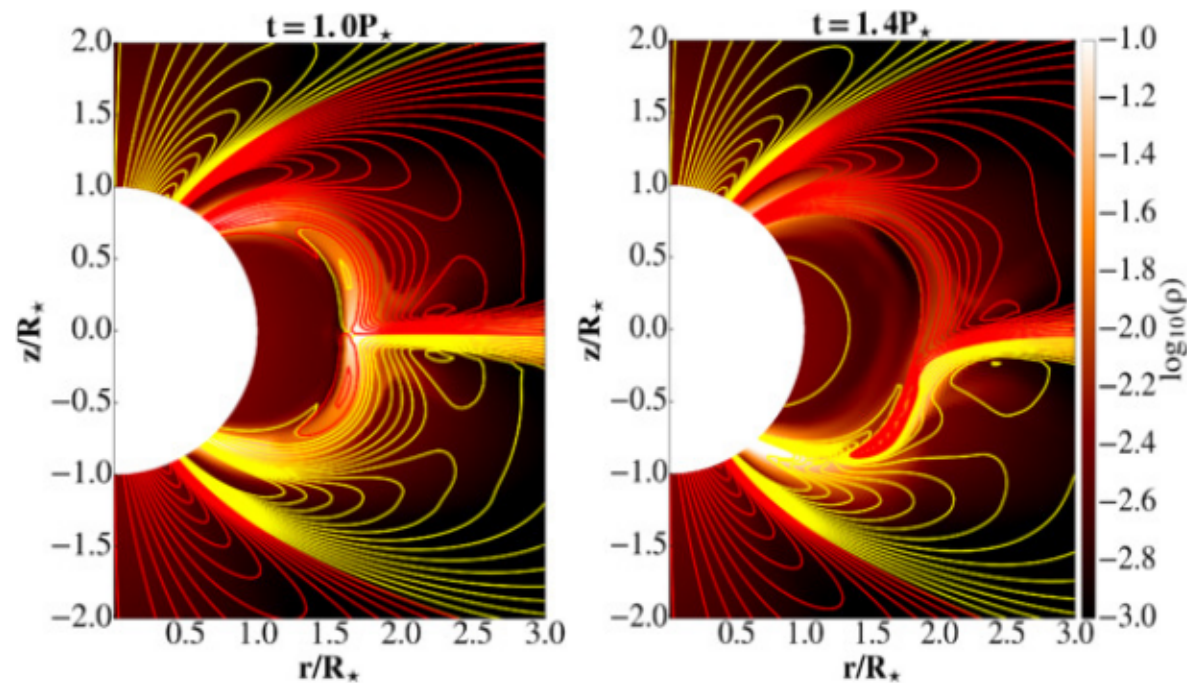


Figure 3. Poloidal current circuits close to the star in our simulation, taken at the same times as shown in Fig. 2, visualized by the isocontours of rB_φ . They are circulating clockwise along the isosurfaces of $rB_\varphi > 0$ (red lines) or counter-clockwise along the $rB_\varphi < 0$ surfaces (yellow lines). The magnetic torque along the red (yellow) lines speeds (slows) the star rotation. Asymmetry in the current circuits supports the switching. The background color represents the density in the units of ρ_{d0} .

Light curve from 3D model with ring-shaped hot spots

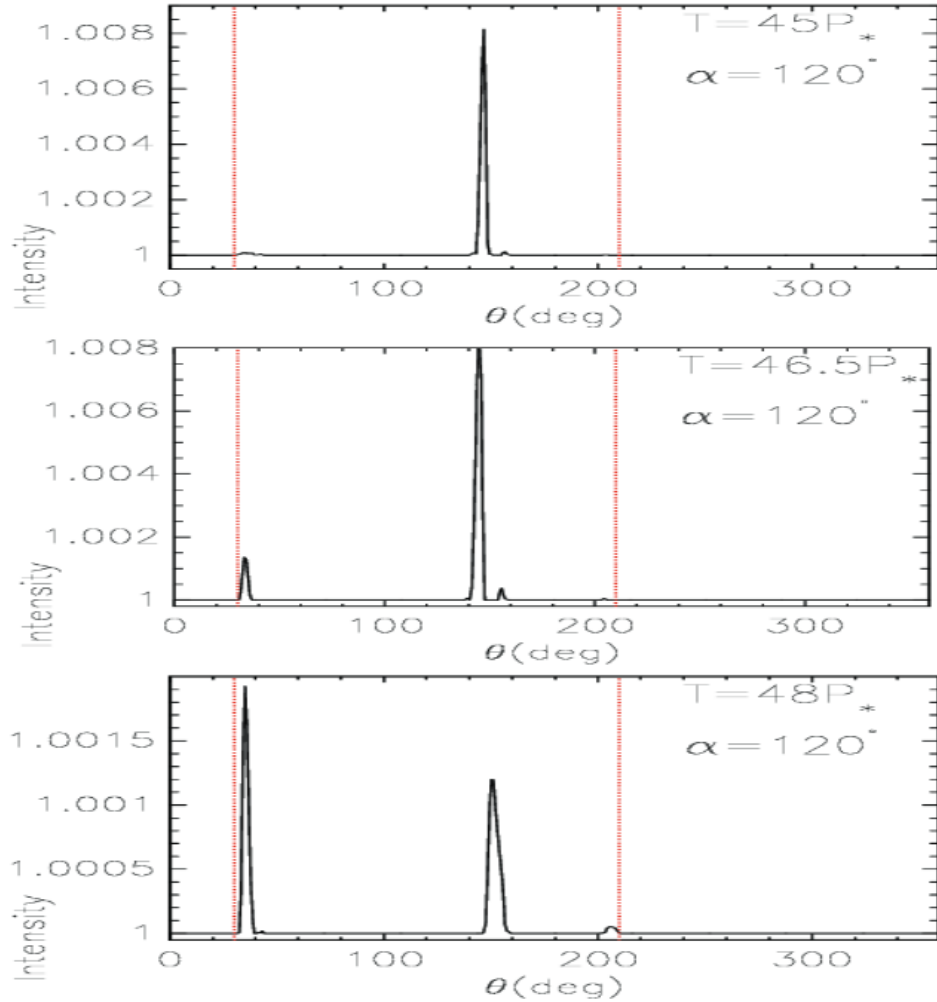


Figure 6. Distribution of the intensity of emission along the meridional direction at times in the simulation shown in Fig. 4, as seen by a distant observer under the angle $\alpha = 120^\circ$, measured from the northern pole. The intensity is normalized by Eq. 6 to the stellar luminosity without hot spots. Width of the rings is of the order 10° or smaller. The part of the stellar surface which is visible to the observer is positioned between the vertical dashed red lines.

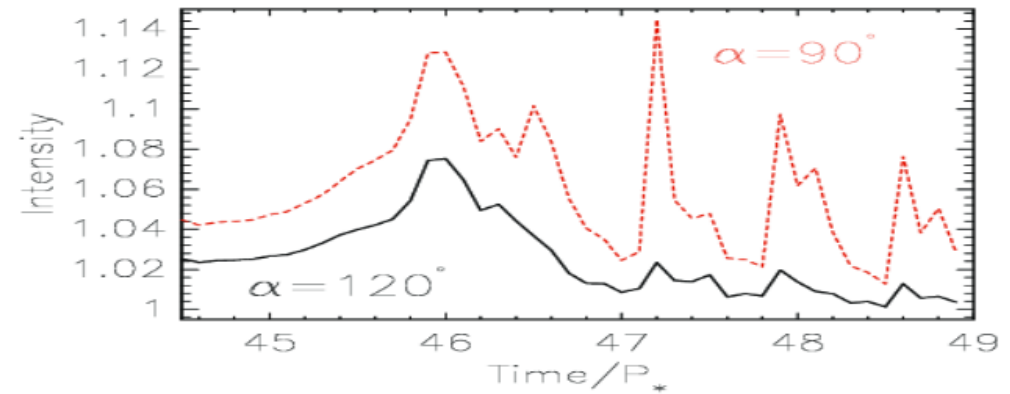


Figure 7. Intensity of the emission in the simulation from Fig. 4, with the ring-shaped hot spots. An observer is positioned at a co-latitudinal angle $\alpha = 90$ (dashed red line) or $\alpha = 120$ (solid line) degrees. Time is measured in the number of stellar rotations.

Comparison with the observational light curve: “hiccup” lasting on the similar time scale!

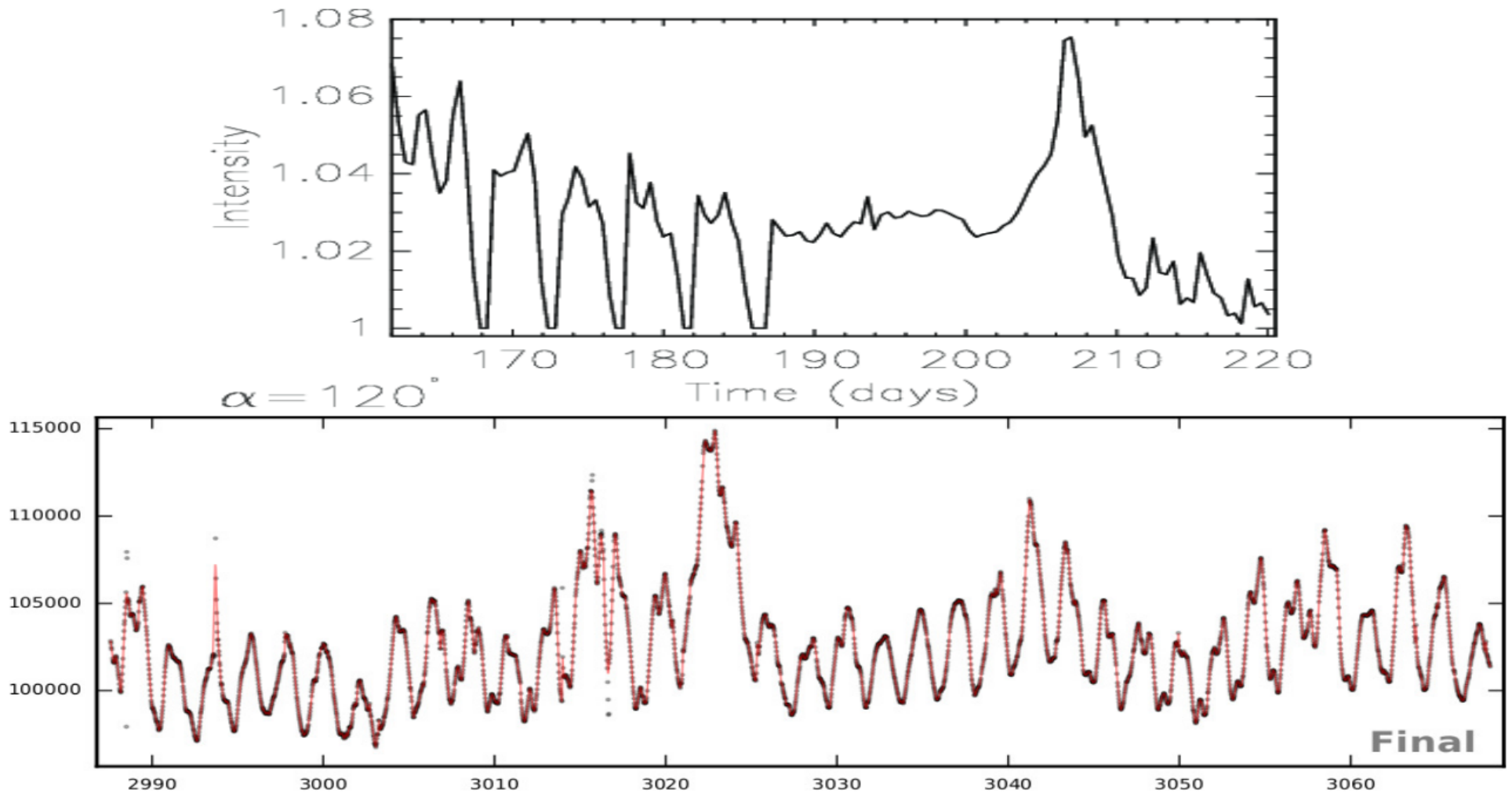


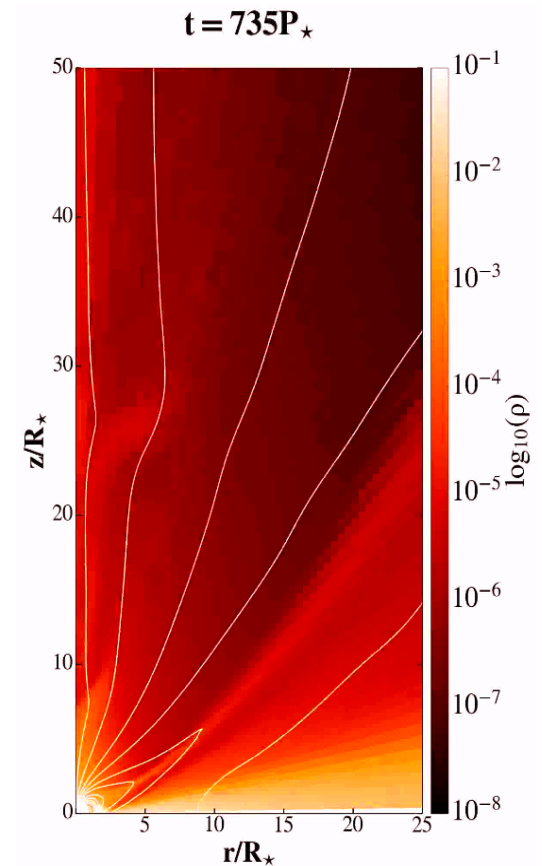
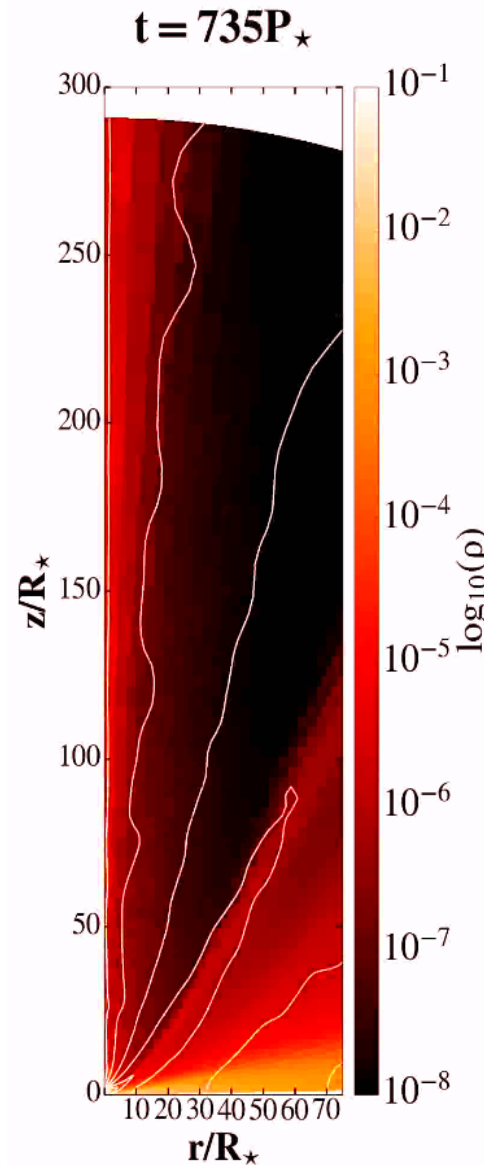
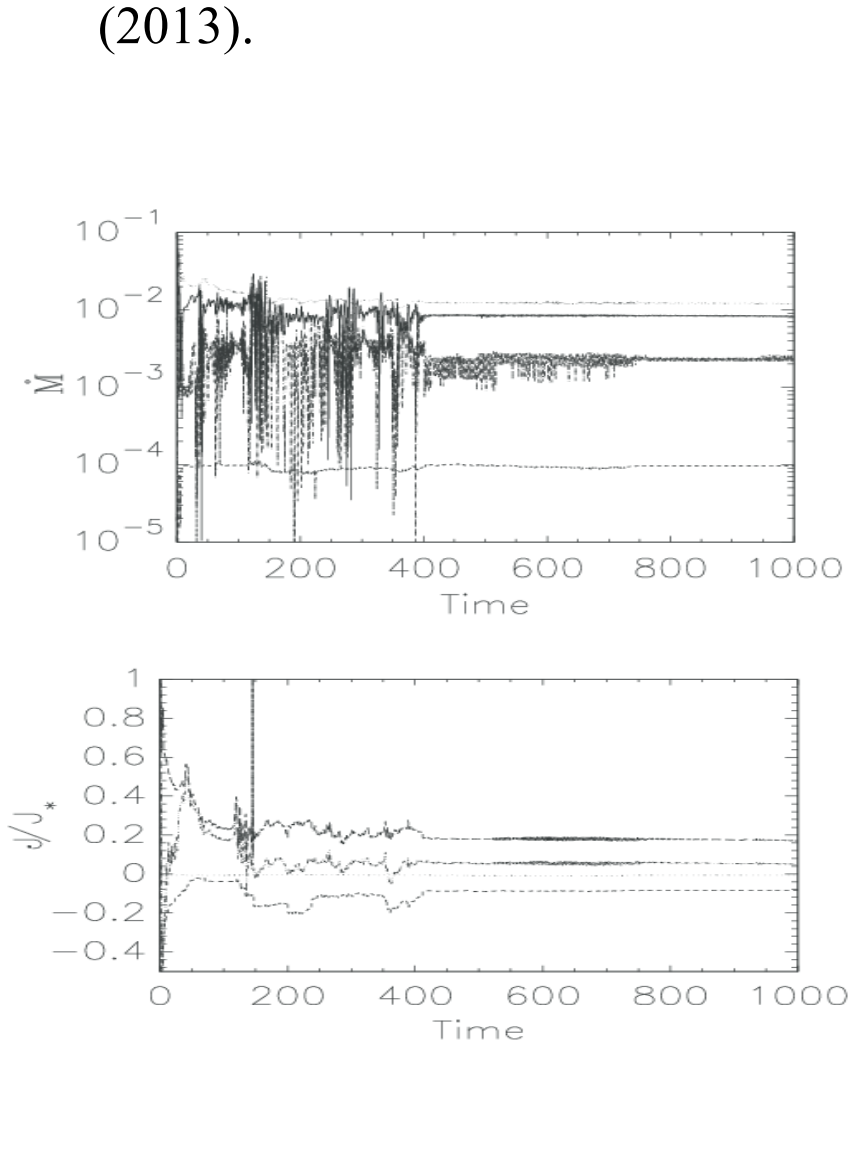
Figure 8. *Top panel:* Intensity in a 3D model made from the longer time sequence than shown in Fig. 7. Shifts in the phase of the observed light (“hiccup”) occur during the switch of the accretion column from the southern to northern stellar hemisphere between the 190 and 210 days. *Bottom panel:* Light curve from the Kepler observation of V1000 Tau in which part of the contribution could occur because of the column switching. Time in the abscissa is annotated in Julian days.

Summary

- I obtained viscous and resistive MHD star-disk magnetospheric interaction solutions for a thin accretion disk.
- A quasi-stationary state is obtained in a set of 64 simulations with slowly rotating stars. With help of students, the sample is increased to more than 100 simulations: with faster rotations ($\Omega_s=0.4,0.7,1$), and also $\alpha_v=0.1,0.4$
- Results are compared, to find trends in solutions.
- In the cases with $\alpha_m=0.1$, conical outflows are launched.
- In the cases with $\alpha_v < 0.68$, we obtain backflows in the disk.
- In the cases with faster rotating stars, axial jets are launched-we study asymmetric axial jet launching.
- As a “free” bonus came the switching of the column footpoint.
- To enable faster parameter studies, I constructed a 3D model from 2D simulations.
- Currently, I am developing a 3D setup of star-disk simulations with the tilted magnetic field with respect to the stellar rotation axis.

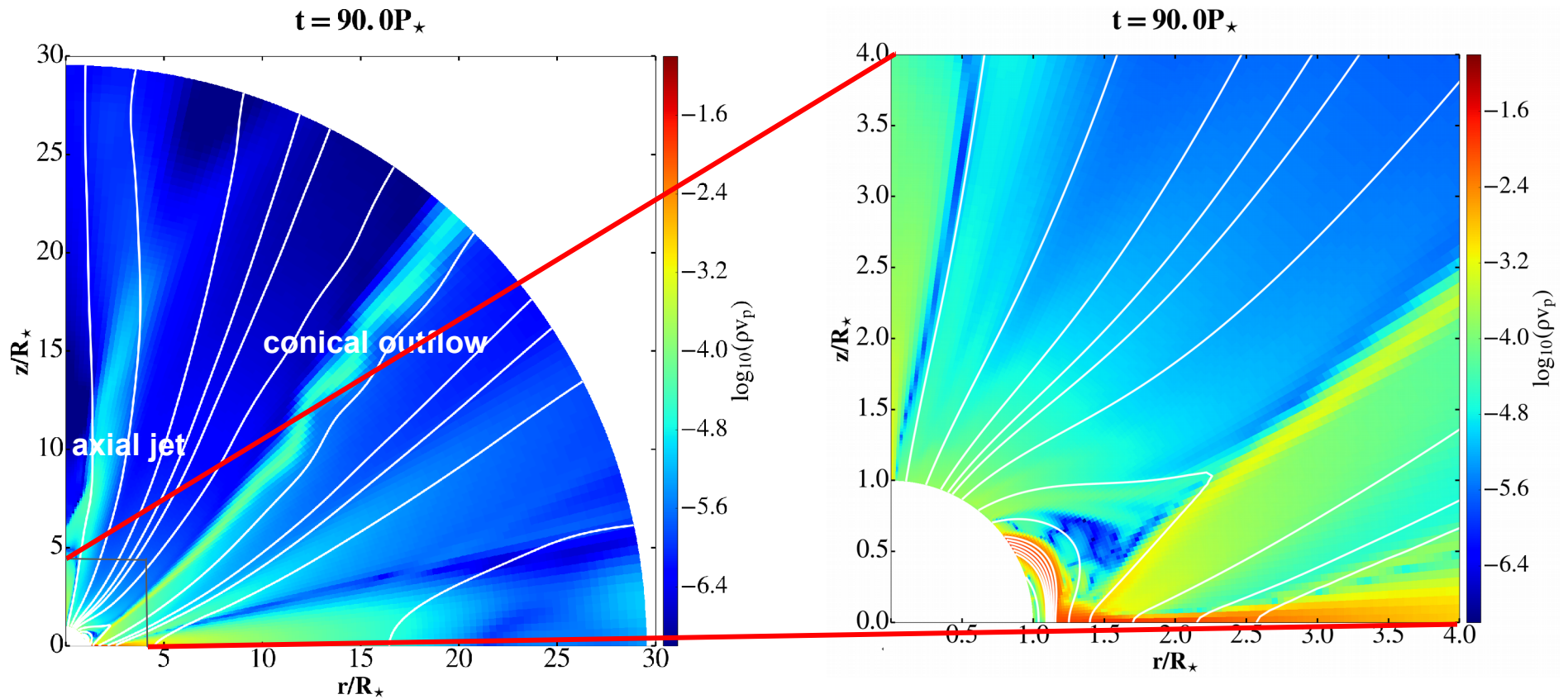
The jet launching

- In a part of the parameter space, there is a continuous launching of an axial jet from the star-disk magnetosphere. In my simulations, it showed that one has to wait until few hundreds of rotations of the star.
- The axial jet and the conical outflow are launched after the relaxation from the initial conditions. They are similar to the results in Romanova et al. (2009) and Zanni & Ferreira (2013).



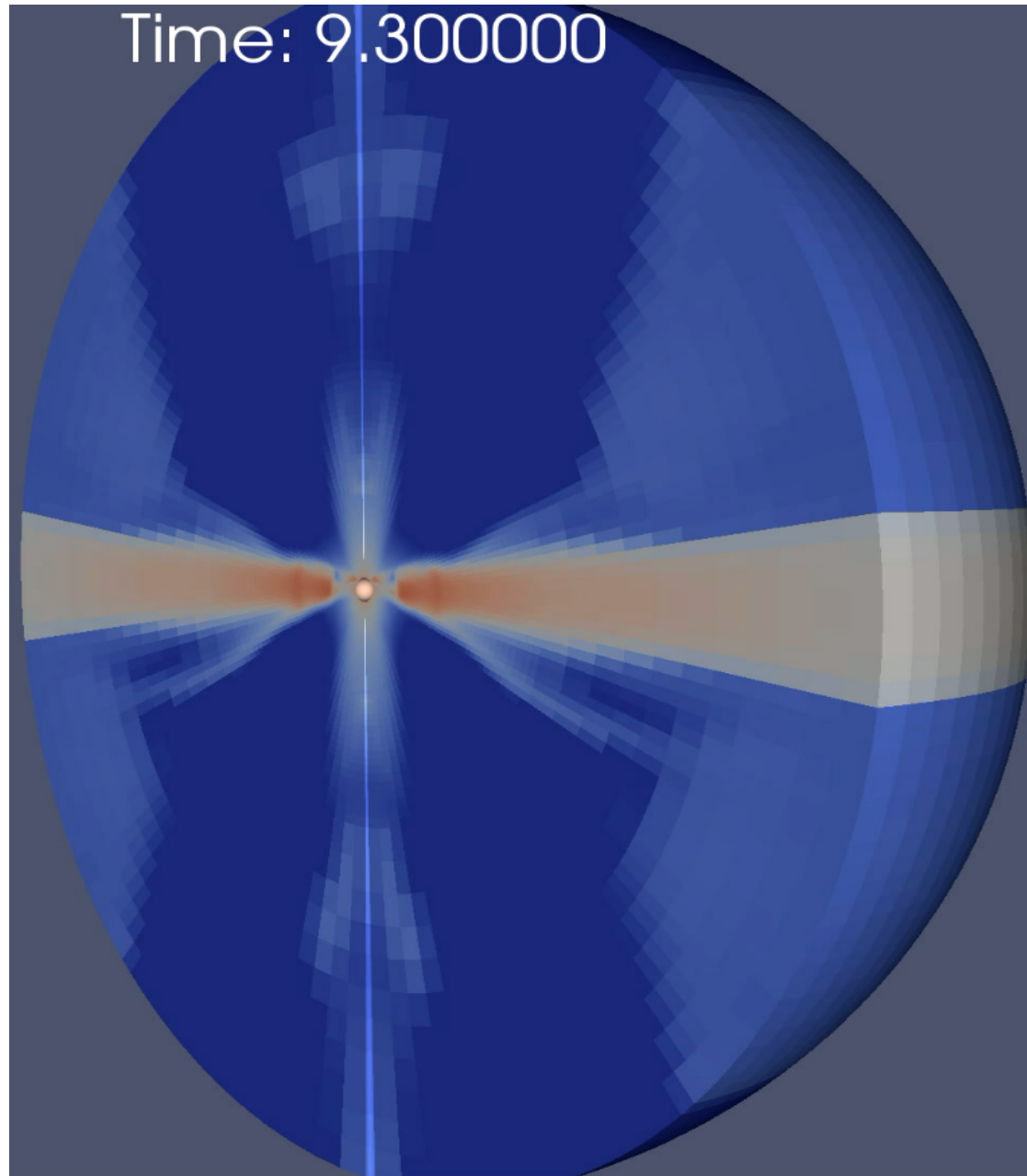
Zoom into the launching region.

Magnetospheric launching of conical outflow and axial jet



Color shows momentum in the MHD simulation in the young stellar object with conical outflow and axial jet, lines are the magnetic field lines. Right panel is a zoom into the left panel close to the star, to show the closest vicinity of the star.

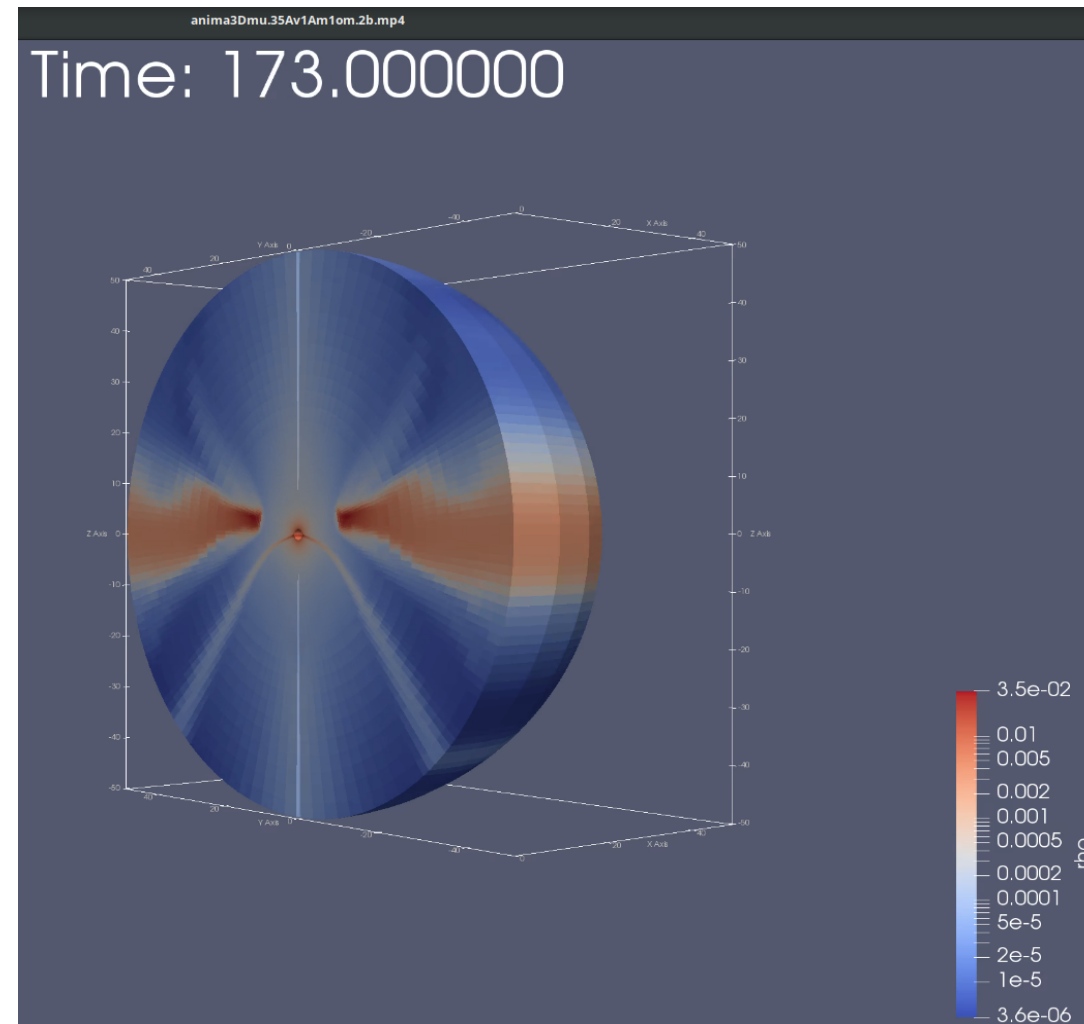
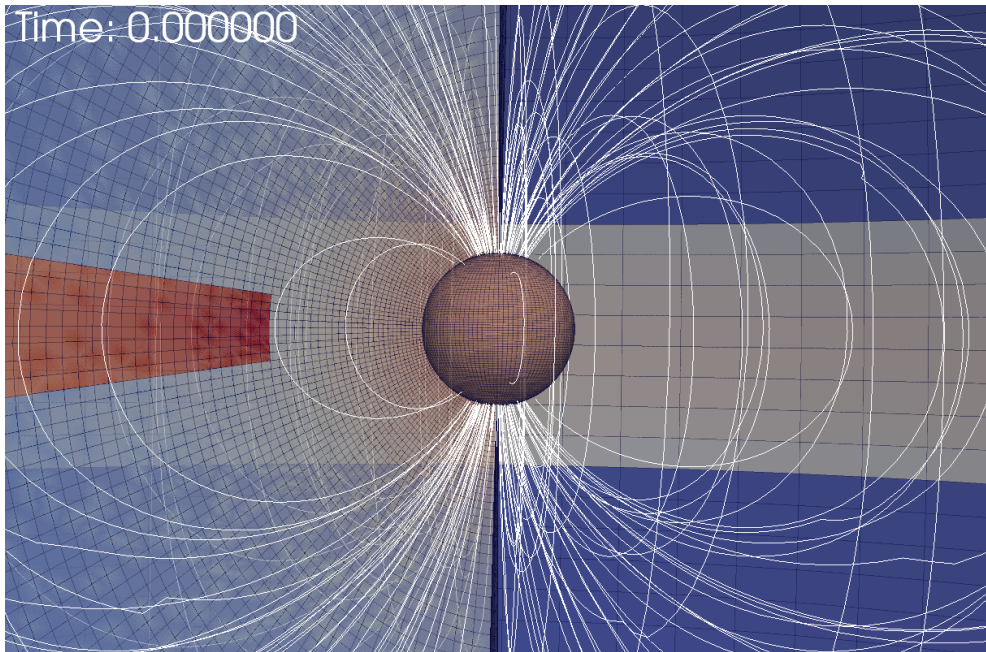
The asymmetric jet launching in 3D simulations



- In the full 3D simulations I also obtain asymmetric jets. To be continued...

3D simulations, case with magnetic field aligned with rotation

- The first step here is to perform the axisymmetric 3D simulation. I use the spherical grid. The magnetic field in this case is aligned with the rotation axis.
- Zoom into the vicinity of the star=inner boundary condition at $T=0$ and at $T=173$



3D simulations, tilted magnetic field case

- The magnetic field in this case is not aligned with the rotation axis.

